ChemSystemsChem

Reviews
doi.org/10.1002/syst.202000026

Chem
Europ
European C
Societies P

Check for
updates

Autocatalysis: Kinetics, Mechanisms and Design

Anton I. Hanopolskyi, Viktoryia A. Smaliak, Alexander I. Novichkov, and
Sergey N. Semenov*[a]
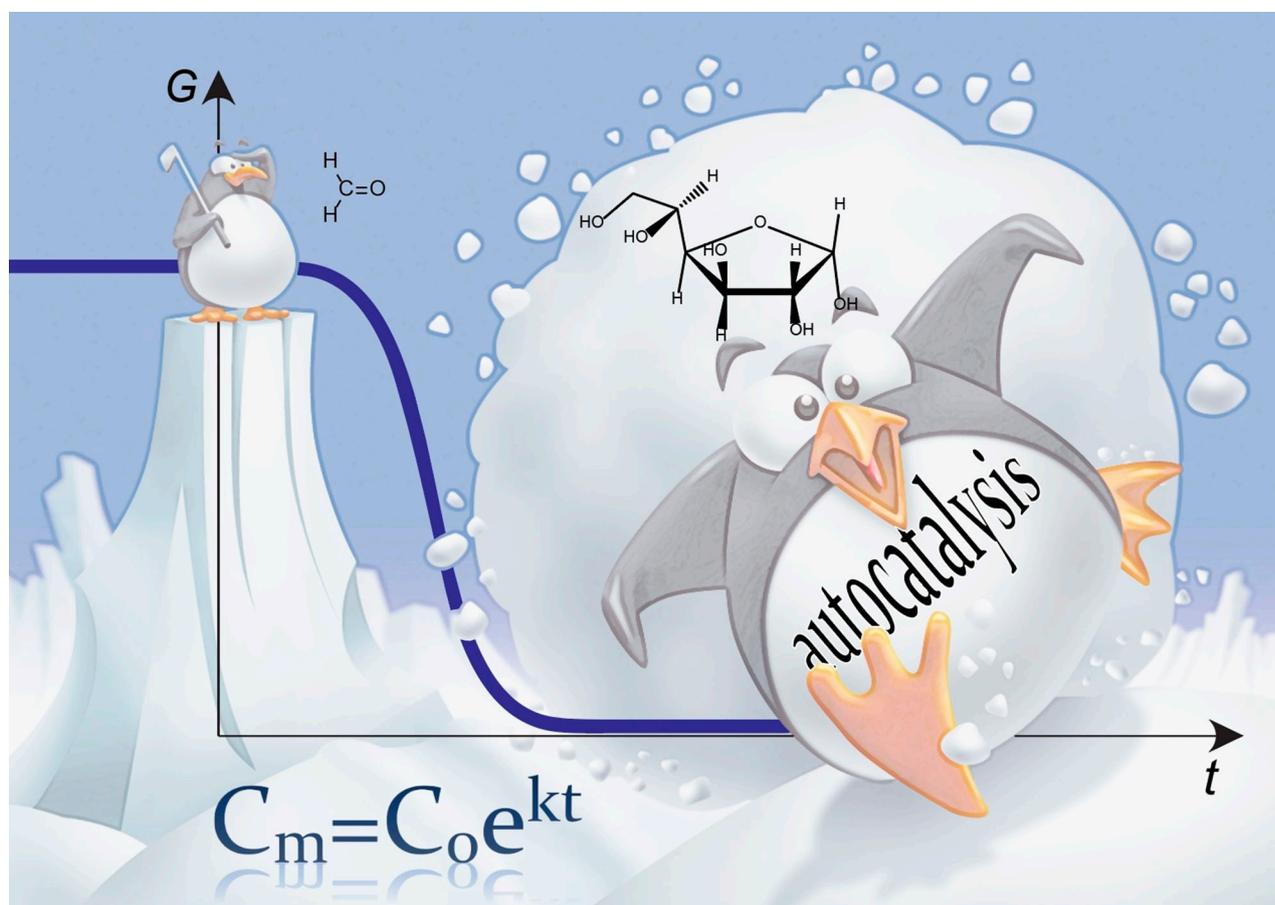
The importance of autocatalysis spans from practical applications such as in chemically amplified photoresists, to autocatalysis playing a fundamental role in evolution as well as a plausible key role in the origin of life. The phenomenon of autocatalysis is characterized by its kinetic signature rather than by its mechanistic aspects. The molecules that form autocatalytic systems and the mechanisms underlying autocatalytic reactions are very diverse. This chemical diversity, combined with the strong involvement of chemical kinetics, creates a formidable barrier for entrance to the field. Understanding these challenges, we wrote this Review with three main goals in mind: (i) To provide a basic introduction to the kinetics of autocatalytic systems and its relation to the role of autocatalysis in evolution, (ii) To provide a comprehensive overview, including tables, of synthetic chemical autocatalytic systems, and (iii) To provide an in-depth analysis of the concept of autocatalytic reaction networks, their design, and perspectives for their development.

1. Introduction

Autocatalysis is a fascinating natural phenomenon in chemistry. In an autocatalytic reaction, the products of the reaction amplify the rate of their production. These products are called autocatalysts. The mechanisms underlying the amplification may vary greatly, but the kinetic signature of isothermal autoamplification is well preserved.[1]

In physics and biology, autoamplified processes play exceptional roles. Nuclear chain reactions are the basis of nuclear energy production. Biological self-replication characterizes all living matter from viruses to humans. Chemistry is somewhat of an outlier, with autocatalytic reactions being more exotic than the core reactions in chemical sciences. Nevertheless, autocatalytic reactions play a key role in industrial processes such as photolithography,[2] electroless plating,[3] and photography.[4] Photolithography, which is a core technology for the microelectronic industry, uses chemically amplified photoresists that are usually based on the autocatalytic formation of acid.[2] Electroless plating uses an autocatalytic reduction of metals (e.g., nickel) on surfaces.[3] In silver bromide photography, the grains of metallic silver, which are generated when photographic film is exposed to light, further catalyze the chemical reduction to colloid silver during the developing stage.[4]

Autocatalysis is a core branch of a new and growing field of systems chemistry.[5] Interest in autocatalysis often comes from its crucial role in theories on the origin of life on Earth.[6] According to the RNA world scenario, life emerged from autocatalytic, self-replicating RNA molecules.[7] Metabolism first scenario proposes the formation of autocatalytic cycles such as a reverse Krebs cycle and the formose reaction.[8] Autocatalysis, as a nonlinear phenomenon, is a source of chemical instabilities (e.g. as in chemical oscillations)[9] and symmetry breaking (e.g. as during formation of patterns in an initially homogenous layer of reactants solution).[10] Therefore, it is of great interest for research on out-of-equilibrium, dissipative chemical systems.[11] An ambitious goal of building synthetic life requires designing complex de novo autocatalytic systems.

The field of autocatalysis encompasses disciplines ranging from chemical kinetics to inorganic and organic chemistry. This broadness of these disciplines creates a substantial barrier for newcomers to the field; therefore, autocatalysis warrants a review with a broad coverage of the topic. There are several excellent thematic reviews in subtopics of template autocatalysis and enantioselective autocatalysis.[12] Nevertheless, the only broad review on autocatalysis that we are aware of is the excellent work from Bissette and Fletcher.[13] In our work, we attempted to cover the majority of the homogeneous, non-biological autocatalytic systems. We skipped the majority of biochemical systems as well as micellar autocatalysis on an oil/water interface.

We wrote this review with three main goals in mind: (i) to provide a basic introduction to the kinetics of autocatalytic systems for a reader not specializing in this area; (ii) to provide a comprehensive overview of the existing autocatalytic reactions; and (iii) to introduce the concept of autocatalytic reaction networks, their design, and perspectives for their development.

2. Kinetics of Autocatalysis

2.1. General Kinetic Signature of Autocatalysis

The isothermal acceleration of the rate of chemical reaction by-products of this reaction, namely, autoamplification, is the universal signature of autocatalysis.[1,14] Autocatalytic reactions can greatly differ in their mechanisms-ranging from the simplest examples such as ester hydrolysis, to extremely complex processes such as the cell cycle. All of these processes are characterized by autoamplification.[1,13] Autoamplification can be mathematically expressed in the form [Eq. (1)]:

$$\frac{d[A]}{dt} = K(A, C) \cdot [A]^n + f(C) \tag{1}$$

with the following conditions [Eqs. (2,3)]:

$$K(A, C) \cdot [A]^n \gg f(C) \tag{2}$$

$$n > 0 \tag{3}$$

Here A is the concentration of an autocatalyst (i.e., a product of the reaction) and C are the concentrations of all compounds other than the autocatalyst in a system. If $K(A,C)$ is a decreasing function from A, then $K(A,C)$ should decrease

[a] A. I. Hanopolskyi, V. A. Smaliak, A. I. Novichkov, Dr. S. N. Semenov
Department of Organic Chemistry
Weizmann Institute of Science
Herzl, 234, 7610001, Rehovot (Israel)
E-mail: sergey.semenov@weizmann.ac.il

ChemSystemsChem

Reviews
doi.org/10.1002/syst.202000026

Chemistry Europe
European Chemical
Societies Publishing

slower than $[A]^n$ increases. In other words, $K(A,C) \cdot [A]^n$ should be an increasing function for any positive A.

The exact form of the kinetic equation will depend on the mechanism of the reaction in question. Plasson et al. published an excellent summary of the relation between the mechanisms of autocatalysis and the resulting kinetics of autocatalytic reactions.[1] Herein we will only touch on some important conclusions and examples.

2.2. Rate Order of Autocatalysis

Many important properties of autocatalytic reactions depend on the "strength" of the autoamplification.[15] To quantitatively characterize the strength of the autoamplification, we need to simplify Equation (1) to the following form [Eq. (4)]:

$$\frac{d[A]}{dt} = K(C) \cdot [A]^n + f(C) \tag{4}$$

With this simplification, the rate of the reaction is a power function of the concentration of A. The steepness of this function is defined by its power n. We need to consider two important consequences of n: the form of the integral $A(t)$ function and the form of the differential equation when the mass balance between products and substrates is taken into account. The integral equations for $n = 1/2$, 1, 2, $K(C) = k$, $f(C) = 0$, and $A(t=0) = A_0$ correspond to parabolic [Eq. (5)], exponential [Eq. (6)], and hyperbolic [Eq. (7)] functions, respectively:

$$A = \frac{k}{4}t^2 + k\sqrt{A_0 t} + A_0 \tag{5}$$

$$A = A_0 e^{kt} \tag{6}$$

$$A = \frac{A_0}{1 - A_0 kt} \tag{7}$$

Figure 1 illustrates how the acceleration of the rate of the production of A depends on the growth function. We would like to highlight two major consequences of different growth functions: (i) the dynamic behavior of the system and (ii) the selection of competitive replicators. The classical example highlighting the difference in the dynamic behavior is the bistability in a continuously stirred tank reactor (CSTR).[11a,16] Exponential autocatalysis does not result in bistability in CSTR in the absence of additional reactions; in contrast, hyperbolic autocatalysis affords bistability in CSTR. The influence of the kinetics of autocatalysis on the selection of competitive replicators will be discussed in the next chapter.

The reader can easily find the terms quadratic and cubic autocatalysis in the literature. These terms should not be confused with exponential and hyperbolic growth, discussed above. They come from a form of differential equations in a situation where there is a limited supply of a substrate. Let us look at two chemical reactions that follow [Eqs. (8,9)]:

$$S + A \xrightarrow{k} 2A \tag{8}$$

Anton Hanopolskyi was born in Zaporizhia, Ukraine. He received an undergraduate degree at Kyiv State University. Currently, he is a M.Sc. student at the Weizmann Institute of Science. He works under the supervision of Dr. Sergey Semenov. The main focus of his research is replication in synthetic systems.

Viktoryia Smaliak was born in Minsk, Belarus. She received her undergraduate degree from Belarusian State University in 2014. She is currently working on her MSc degree at the Weizmann Institute of Science under the supervision of Dr. Sergey Semenov. She is studying the origins of life.

Alexander Novichkov was born in Moscow, Russia. He holds an MSc degree in chemistry Higher Chemical College of the Russian Academy of Sciences. He is currently a PhD student in the Weizmann Institute of Science under the supervision of Dr. Sergey Semenov. The main direction of his studies are the origins of life.

Dr. Sergey Semenov earned a master's degree in chemistry with honors from Moscow State University, Russia in 2006. He earned a PhD in chemistry with honors from the University of Zurich, Switzerland in 2011. He started post-doctoral work in the group of Prof. Wilhelm Huck at the Radboud University of Nijmegen, The Netherlands in autumn of 2010, and became a Marie-Curie fellow in 2012. From 2014 to 2017, he was a postdoctoral scholar in the group of Prof. George Whitesides at Harvard University. In 2018, he became a principal investigator at the Weizmann Institute of Science, Israel. He studies emergent phenomena in nonequilibrium chemical systems.

ChemSystemsChem

Reviews
doi.org/10.1002/syst.202000026

Chemistry Europe
European Chemical
Societies Publishing
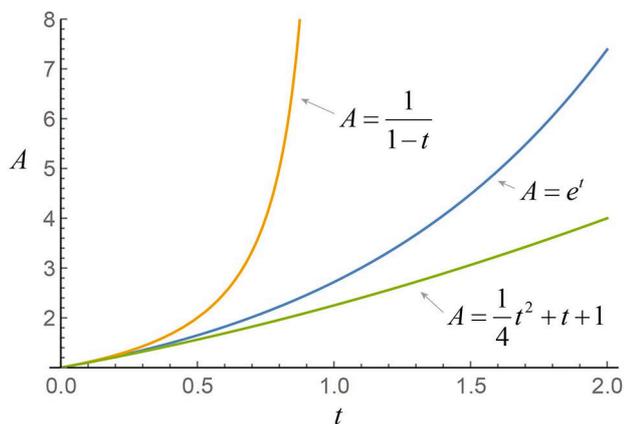
Figure 1. Comparison of the growth rate for parabolic (green), exponential (blue), and hyperbolic (orange) functions from Equations 1.5–1.7 with A0 = 1 and k = 1. The hyperbolic function is plotted only partially because it approaches infinity at t = 1.

$$S + 2A \xrightarrow{k} 3A \tag{9}$$

where A is the autocatalyst and S is the substrate.

Rate equations for producing A have the following forms [Eqs. (10, 11)]:

$$\frac{d[A]}{dt} = k[A][S] \tag{10}$$

$$\frac{d[A]}{dt} = k[A]^2[S] \tag{11}$$

As one can see, the equations are first- and second-order on A. Nevertheless, the concentrations of A and S are not independent because A is produced from S. They are connected through the mass balance equation [Eq. (12)]:

$$[A] + [S] = [A_0] + [S_0] = C_0 \tag{12}$$

Substituting S for C_0–A results in Equations (13) and (14):

$$\frac{d[A]}{dt} = k[A]C_0 - k[A]^2 \tag{13}$$

$$\frac{d[A]}{dt} = k[A]^2[C_0] - k[A]^3 \tag{14}$$

They are quadratic and cubic on A.

2.3. Basic Analysis of Experimental Kinetics of Autocatalytic Reactions

Importantly, integrating equation 13 with $A(t=0)=A_0$ results in a sigmoidal function [Eq. (15)]:

$$A = \frac{C_0}{1 + \frac{(C_0 - A_0)}{A_0} e^{-C_0 kt}} \tag{15}$$

This function has three characteristic regions: (i) the lag phase, (ii) the exponential phase, and (iii) the saturation phase (Figure 2).[17]

The regions are not sharply defined. Tentatively, the lag phase is the region where only a small fraction of starting material is converted to the product; exponential phase is the region from the lag phase to the bending point of the sigmoidal curve where the acceleration of the reaction rate is evident; saturation phase is the region from the bending point to the completion of the reaction. Because many experimental autocatalytic systems are exponential and substrates are always in limited supply in experiments, sigmoidal kinetics is usually expected from autocatalytic reactions and is the first experimental sign of autocatalysis. Nevertheless, other processes (e.g., the accumulation of an intermediate) can cause a lag phase. Thus, to prove the autocatalytic nature of a reaction, we need to demonstrate that its rate increased with the addition of products. This is usually done by measuring the initial reaction rate with increasing initial concentrations of products.[18]

2.4. Motifs of Autocatalytic Reaction Networks

The difference between an autocatalytic reaction network and an autocatalytic reaction with a complex mechanism is ambiguous. Usually, we refer to an autocatalytic reaction with a complex mechanism in situations when the reaction intermediates are short living and cannot be separated as individual compounds. The autocatalytic oxidation of oxalic acid by permanganate is an example of an autocatalytic reaction with a complex mechanism.[19] We refer to autocatalytic reaction networks when the intermediates are stable, separable compounds; usually they are important independent of the context of the mechanism underlying a particular reaction. The formose reaction – the autocatalytic formation of sugars from formaldehyde – is an example of an autocatalytic reaction network.[8c,20]
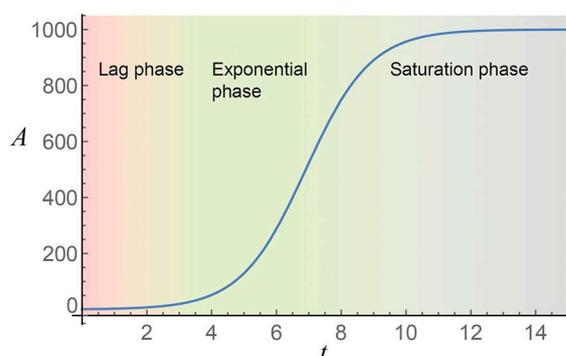
Figure 2. The plot of function (15) with k = 0.001, C_0 = 1000, and A_0 = 1.

ChemSystemsChem

Reviews

doi.org/10.1002/syst.202000026

Chemistry Europe

European Chemical
Societies Publishing

Theoretically, the number of autocatalytic reaction networks, and for that matter, autocatalytic mechanisms, is unlimited. Motifs that are likely to be formed from real chemical reactions were studied theoretically (Figure 3).

The simplest motif is direct autocatalysis (Figure 3a); however, it can involve many stable intermediates and still represent a complex reaction network as in the reverse Krebs cycle.[8a,b] Hinshelwood's paper on cyclic mutualistic catalysis (Figure 3b) is perhaps the first example of an analysis of the kinetics of an indirect autocatalytic network where products do not directly catalyze their production but catalyze the formation of catalysts for their production.[21] Hinshelwood's paper concludes that, independent of a number of catalysts in the cycle (e.g., three in Figure 3b), the system approaches exponential growth after some lag period during which transient oscillatory behaviors are possible. Often, the autocatalytic network does not involve a series of catalysts – only one catalyst and a series of non-catalytic intermediates (Figure 3c). Semenov and Skorb showed that thioester autocatalysis,[22] some variants of azide-alkyne autocatalysis[23] and the formaldehyde sulfide reaction[24] all belong to this type of network structure.[25] This network always results in exponential growth after some lag phase where growth is slower than an exponential rate.

All reaction networks from Figure 3 display exponential growth. Examples of reaction networks resulting in parabolic and hyperbolic growth are rarer than exponential systems. A notable example of a parabolic system is a template replication with strong product inhibition through the formation of a dimer (Figure 4a).[18,26] The equilibrium between an active monomeric autocatalyst and an inactive dimer should be almost fully shifted toward the dimer for parabolic kinetics; if the equilibrium is shifted toward the monomer, the system will show exponential kinetics.[27] Sexual reproduction is an example of a hyperbolic system. Chemical reactions rarely display hyperbolic growth. Most likely, candidates for experimentally realizable
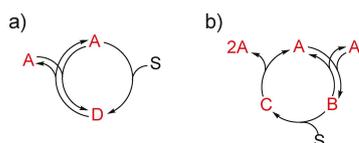
reaction networks with hyperbolic dynamics involve the formation of an active catalyst through the dimerization step (Figure 4b). A variation of this network with the stepwise formation of the dimer displays dynamics that characterize hyperbolic systems.[28]

2.5. Limitations of the $[A]^n$ Approximation

The order of autocatalysis is not an intrinsic property of a reaction. An exact kinetic rate equation might have a form that in one stage of the reaction it will display parabolic growth, whereas at other stages it will display exponential growth. Let us look at the following example [Eq. (16)]:

$$\frac{d[A]}{dt} = \frac{k_1[A]}{k_2 + [A]} \tag{16}$$

This equation might represent an autocatalytic production on an enzyme with product inhibition. During the initial stages of the reaction, when $[A]$ is low, $k_2 \gg [A]$, and growth is exponential; during the intermediate stages $k_2 \approx [A]$ and growth is parabolic; during the late stages $k_2 \ll [A]$ and growth is linear. Finally, even the general equation 1 is sometimes inappropriate to describe the growth dynamics. Let us imagine a replicator that increases "fertility" with each replication cycle. Thus, division occurs, let's say, every hour, but during the first division cycle a mother cell produces one daughter cell, during the second division cycle two daughter cells, and so on. The growth is faster than the exponential growth, but it is not hyperbolic; it is actually factorial (Figure 5).

2.6. Autocatalytic Closure

Kaufmann introduced the term "autocatalytic closure" during the development of the theory of autocatalytic sets.[29] The meaning of this term and its implications were explicitly discussed by Plasson and indirectly highlighted by Blackmond.[1,30] In simplified form, the point is that autocatalytically closed reactions should produce all products and catalysts that are required for these reactions from the initially defined set of starting materials. Thus, Blackmond points out that if catalysts for a reaction is a limiting resource, the reaction will not sustain autoamplification even if the starting materials would be constantly supplied.[30] Plasson showed how to calculate the property of autocatalytic closure from stoichio-

Figure 3. Examples of autocatalytic reaction networks with exponential growth. S denotes the substrate, red letters denote catalytic species, and blue letters denote non-catalytic intermediates.

Figure 4. Examples of autocatalytic reaction networks with parabolic (a) and hyperbolic growth (b). An intermediate D in the parabolic system is often a dimer of A, [A·A]. An intermediate B in the hyperbolic system could be an active enzyme formed from two inactive subunits.

Figure 5. An example of factorial growth.

ChemSystemsChem

Reviews
doi.org/10.1002/syst.202000026

Chemistry Europe
European Chemical
Societies Publishing

metric matrices.[1,31] The importance of autocatalytic closure becomes apparent in an open system where reactants are constantly supplied, and products are constantly removed. If one of the compounds (e.g., a catalyst) is not produced from the supplied reactants, the autoamplification will fade away because of the removal of this limiting compound.

2.7. Role of Noncatalytic Reactions

Any catalytic reaction is accompanied by a direct, non-catalytic transformation from reactants to products. The non-catalytic pathway could be negligible, but it always exists. The same principle applies to autocatalytic reactions; they are always accompanied by the direct non-catalytic transformation of reactants to products. Importantly, with an autocatalytic reaction, the products formed in the direct reaction initiate the autocatalytic process. The contribution of the direct reaction to the overall production of products is an important characteristic of a particular autocatalytic reaction. If the contribution of the direct reaction is too strong, the dynamic effects of autocatalysis will be masked; the system properties emerging from autocatalysis such as Darwinian selection,[25] bistability, propagation of the reaction front, and oscillations will not appear.[11a] Let's consider the simplest example of an autocatalytic reaction:

$$S + A \xrightarrow{k_1} 2A$$
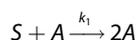
This reaction will always be accompanied by a direct reaction:

$$S \xrightarrow{k_2} A$$

We cannot directly compare the rate constants of these reactions because one of them is first-order, whereas another is second-order. Thus, we will compare the reaction rates in the middle of the reaction when half of the substrate S is consumed. When autocatalysis is only twice as fast as the direct reaction, the sigmoidal character of the kinetic curve is absent; even when the difference is tenfold, the kinetics is only slightly different from a typical first-order reaction; however, when the difference is a hundredfold, the sigmoidal kinetics is clear (Figure 6). This quantitative difference in the kinetic behavior for different rate ratios of autocatalytic and direct reactions translates into the qualitative difference between the presence and absence of emergent dynamic phenomena (e.g., oscillation and patterns). The importance of the ration between rates of autocatalytic and non-catalytic pathways was highlighted by Von Kiedrowski. He states that the self-replicating success of the system may be measured by the template molecule's catalytic efficiency and reaction order.[26b–d] Catalytic efficiency is defined as the rate of the autocatalytic reaction of the intermolecular template's reactant complex, over the rate of the "background" reaction – the reaction of the non-templated coupling of trinucleotides. The increase in the rate of the background reaction decreases the catalytic efficiency.
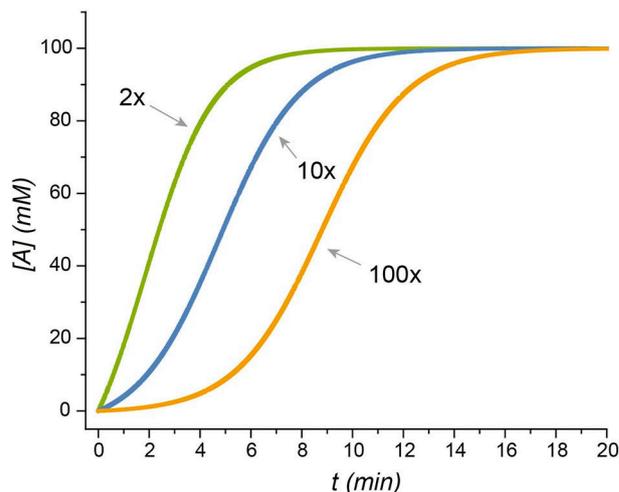
Figure 6. Influence of the direct non-catalytic reaction on the kinetics of the formation of an autocatalyst (A). We used the following parameters for the simulation: $S_0 = 100$ mM, $A_0 = 0$, $k_1 = 0.0001$ mM^{-1} s^{-1}, and $k_2 = 0.0025$ s^{-1} (green); 0.0005 s^{-1} (blue); 0.00005 s^{-1} (orange).

We notice that special care should be taken about units of rate constants when comparing autocatalytic and non-catalytic pathways. While non-catalytic pathways are usually associated with first- or second-order reactions with rate constants in time^{-1} or concentration^{-1}time^{-1}, the autocatalytic pathways often display fractional rate orders with rate constants in concentration^{-n}time^{-1} where n can be a fraction.

2.8. Role of Autocatalysis in Chemical Evolution

Autocatalysis is the driving force of evolution because it allows the fittest species to multiply quickly from small to large numbers. Many theoretic works from Eigen,[32] Szathmary,[26a,33] Schuster,[32b–d,34] Lifson,[27,35] Dyson,[36] Lancet,[37] Hordijk,[38] and others were dedicated to study various mechanisms of evolution and the role of autocatalysis in them. This section does not aim to cover these works comprehensively; rather, it aims to highlight key ideas from these works in light of designing a synthetic evolvable chemical system. The work by Eigen was the first and perhaps the most comprehensive treatment of molecular evolution by chemical kinetics[32a] We will illustrate the key ideas of this work by analyzing its main equation [Eq. (17)]:

$$\frac{dx_i}{dt} = (F_i - R_i)x_i + \sum_{j \neq i} \varphi_{ij} x_j \tag{17}$$

This equation describes the kinetics of the production and consumption of chemical replicators $x_1 \ldots x_i$. F_i is a function characterizing the autocatalytic production of x_i. It can be a constant in the simplest case of exponential growth or might depend on x_i. If it depends on x_i in power -1 to 0, the growth is subexponential (e.g., parabolic); if it depends on x_i with a power higher than 0, the growth is superexponential (e.g., hyperbolic).

ChemSystemsChem

Reviews
doi.org/10.1002/syst.202000026

Chemistry Europe
European Chemical
Societies Publishing

The value R_i is a function characterizing the consumption of x_i. It is often a constant because most of the degradation reactions, as well as the washout processes in well-mixed systems are the first order in a substrate. The last sum term describes cross-catalytic processes. It follows that ϕ_{ij} is a function characterizing production of x_i because of catalysis by x_j. Let's examine in detail a case where F_i is a constant. Eigen splits F_i into three terms: [Eq. (18)]:

$$F_i = k_0 \cdot A_i \cdot Q_i \tag{18}$$

where k_0 is a generic first-order rate constant. It keeps A_i and Q_i dimensionless; A_i is the autocatalytic efficiency and Q_i is a quality factor that takes values between 1 and 0. It reflects the quality of information coping; in other words, it reflects the selectivity of an autocatalytic reaction. If it equals 1, the autocatalysis is absolutely specific; if it is less than 1, then x_i has some cross catalytic activity. We note that Eigen's autocatalytic efficiency, which is related to the rate constant for the autocatalytic reaction, is not identical to Kiedrowski's autocatalytic efficiency, which is related to the ration of the rates of autocatalytic and non-catalytic pathways.

The splitting of F_i into A_i and Q_i reflects an important idea – both the efficiency and selectivity of autocatalysis are important for a chemical system to evolve. Autocatalytic efficiency is responsible for exponential (or other accelerated) growth; it has to be higher than the decomposition term R_i. Importantly, equation 17 completely neglects direct, non-catalytic production of x_i. This approximation is valid for highly efficient enzymatic replication in biological cells; however, as we discussed in previous sections, it is unrealistic for the chemistry of small molecules. Thus, an important role of autocatalytic efficiency is to ensure that the autocatalytic production of x_i dominates over direct synthesis. We will illustrate the importance of A_i and Q_i using two examples: (i) synthetic template replicators and (ii) an autocatalytic thiol-thioester network. Templated replication has good selectivity and consequently, a high Q_i value; however, it often has low autocatalytic efficiency and a high reaction rate of the non-catalytic pathway.[26b] The autocatalytic thiol-thioester network,[22] on the other hand, has high autocatalytic efficiency, but a low Q_i value because every thiol in this system cross-catalyzes the production of other thiols. Therefore, the goal is to find experimental systems with both high A_i and Q_i values.

Let us look at how the character of F_i influences the selection process. Szathmary,[33b,39] Schuster,[32b–d,34c] Lifson,[27] and others studied this question in detail; we will only outline the main conclusions. If F_i is constant, we deal with exponential replication. In this situation, the replicator x_i with the highest F_i value will extinguish all competitors. However, if Q_i is lower than some threshold, no selection is possible; all replicators grow collectively. This phenomenon is known as an error threshold paradox. If F_i contains $x_i^{-1/2}$, we deal with parabolic replicators. In general, parabolic replication results in the survival of everyone and no selection. If F_i contains x_i, we deal with hyperbolic replicators. For these replicators, survival depends not only on F_i but also on the initial concentration.

This dependency means that once a replicator x_i is dominant, it is very hard for another replicator to extinguish it and gain dominance. A hypercycle is a hypothetical reaction network with hyperbolic growth. The reader can find a detailed description of the hypercycle model in the works of Eigen and Shuster,[34] but it is important to remember that the mandatory characteristic of any hypercycle is hyperbolic growth.

Finally, we will look at the possible chemical nature of replicators x_i. Eigen's theory was developed with the idea that x_i is an information polymer, perhaps RNA. For that reason, the theory is most applicable to the evolution of information polymers. Nevertheless, other chemical entities could be competitive replicators. Kauffman and later Hordijk developed the theory of autocatalytic sets.[29a,38b,e,40] They showed that although in general, autocatalytic reaction networks are incapable of evolution, a subclass of autocatalytic networks with independent autocatalytic cores could evolve.[38b,33c] In essence, these autocatalytic subnetworks (cores) are the competing replicators x_i. Lancet developed these ideas to apply them to the cross-catalytic formation of micelles.[37a,b,d,c] The information in this network of interacting micelles lies in the composition of these micelles, but it cannot be calculated simply from the number of possible compositions. It depends on the number of possible alternative compositions forming independent autocatalytic cores. This requirement for having many orthogonal autocatalytic compositions is, in our opinion, one of the major obstacles in developing experimental evolvable autocatalytic networks.

3. Autocatalysis Based on Inorganic Chemistry

The essential inorganic autocatalytic reactions are summarized in Table 1. Wherever possible, we provided the rate constants for the autocatalytic and background reaction so that readers can assess the efficiency of this autocatalysis.

Probably, autocatalysis was initially discovered among inorganic reactions. The mechanisms underlying such reactions are frequently complicated having, large numbers of transformations that can include red-ox steps, reactions on colloidal surfaces, and radical-based reactions. The systematization of these reactions is a challenging task. Yet we can distinguish the few common classes of these reactions: manganese-based reaction, halogenate- and pseudohalogenate based reactions, reaction with nitrous acid as an autocatalyst, Co^{2+}-based reactions, and reactions involving nanoparticles.

Launer proved the autocatalytic character of the permanganate-oxalate reaction [Eq. (19)].[19a]

$$2MnO_4^- + 6H_3O^+ + 5H_2C_2O_4 \rightarrow 2Mn^{2+} + 14H_2O + 10CO_2 \tag{19}$$
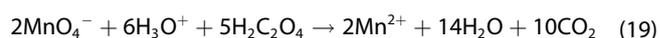
Accordingly to the proposed mechanism, the Mn^{2+} species in the reactions facilitate $KMnO_4$ reduction, which forms MnO_2. Colloidal MnO_2 also reacts with Mn^{2+}, producing Mn^{3+}. Oxalate reduces the Mn^{3+} species to the final Mn^{2+} product[17] (Figure 7(a)). Kovács and co-authors suggested an alternative mechanism, where the formation of MnO_2 colloids initiates

Table 1. Essential inorganic autocatalytic reactions.

Reaction	Autocatalyst	$k_{autocat}$	k_{noncat}	Ref.
$2MnO_4^- + 6H_3O^+ + 5H_2C_2O_4 \rightarrow 2Mn^{2+} + 14H_2O + 10CO_2$	Mn^{2+}	$5*10^3$ $M^{-1}s^{-1}$	$2*10^{-2}$ s^{-1}	[19b, 19a]
$2MnO_4^- + 5HCOOH + 6H^+ \rightarrow 2Mn^{2+} + 5CO_2 + 8H_2O$	Mn^{2+}	0.124 ± 0.004 $M^{-1}s^{-1}$	$1.1*10^{-4}$ s^{-1}	[42]
Permanganate oxidation of glycine/alanine	MnO_2 colloids	Glycine: 1.92 $M^{-1}s^{-1}$ Alanine: 0.214 $M^{-1}s^{-1}$	$4.79*10^{-5}$ s^{-1} $2.98*10^{-5}$ s^{-1}	[44]
				[45]
Belousov-Zhabotinski reaction	$HBrO_2$			[46]
$(1+3x)Co(III) + N_2H_4 \rightarrow (1+3x)Co(II) + N_2 + \frac{1}{2}*(1-x)(N_2 + 2NH_3)$	Co^{2+}	$4.9*10^2$ $M^{-1}min^{-1}$	$2.6*10^{-2}$ min^{-1}	[63]
Figure 8(c)	Co^{2+}			[48]
$3Fe^{2+} + 4H^+ + NO_3^- \rightarrow 3Fe^{3+} + 2H_2O + NO$	NO, HNO_2			[51]
$3NO_3^- + SCN^- + H_3O^+ \rightarrow 3HNO_2 + SO_4^- + CN^-$	HNO_2			[55]
$NO_3^- + 2Br^- + 3H^+ \rightarrow Br_2 + HNO_2 + H_2O$	HNO_2			[53]
$2NO_3^- + 4NH_2OH + 2H^+ \rightarrow 3$ $N_2O + 7H_2O$	HNO_2			[56]
$3H_3AsO_3 + 2HNO_3 \rightarrow 3H_3AsO_4 + 2NO + H_2O$	HNO_2			[54]
$ClO_2^- + 4H^+ + 4Br^- \rightarrow Cl^- + 2Br_2 + 2H_2O$	Br_2			[58]
$H_2PtCl_6/Al_2O_3 + 2H_2 \rightarrow 1/n$ $Pt(0)/Al_2O_3 + 6HCl$	$Pt(0)$	$1.2(2)*10^4$ $h^{-1}M^{-1}$	$2.7*10^{-5}$ h^{-1}	[65]
$6ClO_2 + 5SCN^- + 8H_2O \rightarrow 6Cl^- + 5SO_4^{2-} + 5CN^- + 16H^+$	$OSCN^-$			[60]
$5ClO_2 + 2I_2 + 2H_2O = 5Cl^- + 4IO_3^- + 4H^+$	ICl			[59]
Oligomerization of NH_2BH_2 with Ammonia-Borane	NH_2BH_2			[66]
2 $Ag_2O \rightarrow 4$ $Ag(0) + O_2$	$Ag(0)$			[67]
$4Br_2 + CS(NH_2)_2 + 5H_2O \rightarrow 8Br^- + CO(NH_2)_2 + SO_4^{2-} + 10H^+$	Br^-	$(3.17 \pm 0.3)*10^3$ $M^{-2}s^{-1}$	$2.8*10^1$ $s^{-1}M^{-1}$	[61]
$300[(1,5-COD)Ir*P_2W_{15}Nb_3O_{62}]^{8-} + 750H_2 \rightarrow 300CO + Ir(0)_{300} + 300[P_2W_{15}Nb_3O_{62}]^{9-} + 150H^+$	Ir nanoclusters	$2.14*10^3$ $M^{-1}h^{-1}$	$5.6*10^{-4}$ h^{-1}	[68]
$Fe^{3+} + NBE + HP \rightarrow$ multiple products	$*OH$			[69]
	Mn^{2+}	$3650.0*10^5$ $M^{-1}s^{-1}$	11.4 s^{-1}	[70]
	$NOSCN$	17.8 ± 0.8 $M^{-2}s^{-1}$	$1.1*10^{-2}$ $M^{-1}s^{-1}$	[62]
Molybdenum nanoclusters (Mo_{36}) nanoclusters formation	Molybdenum clusters			[71]
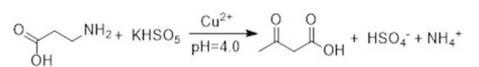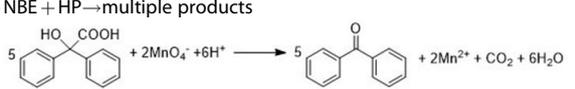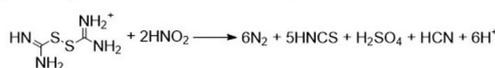
oxalate oxidation.[41] The reactions of $KMnO_4$ with formic acid,[42] glycine,[43] and L-alanine[44b] are all autocatalytic. MnO_2 colloids are autocatalytic in the oxidation of glycine[43] and L-alanine.[44b] The mechanism underlying the oxidation of 2-hydroxy-2,2-diphenylacetic acid with potassium permanganate differs from previous examples. The oxidation occurs through the formation of the complex of manganese (II) and 2-hydroxy-2,2-diphenylacetic acid, which is easier to oxidize by permanganate than by free 2-hydroxy-2,2-diphenylacetic acid.[45]

The Belousov-Zhabotinski reaction is the most famous oscillatory reaction; it employs autocatalysis in the core of its mechanism.[9] Although the overall mechanism is complex, with up to 80 possible elementary steps,[46,47] the autocatalytic core consists of only a few steps. Autocatalysis is initiated by a slow reduction of BrO_3^- to $HBrO_2$ by bromide anions.[9a] Then, $HBrO_2$ reacts with BrO_3^-, forming Br_2O_4 [Eq. (20)].

$$HBrO_2 + HBrO_3 \rightarrow Br_2O_4 + H_2O \qquad (20)$$

The Br_2O_4 formed dissociates into two BrO_2^* radicals, which are reduced into two $HBrO_2$ molecules in the cerium-catalyzed reaction with bromomalonic acid (Figure 7(b)). Thus, $HBrO_2$ is the autocatalyst in the Belousov-Zhabotinski reaction. Although

modifications of the Belousov-Zhabotinski reaction use Fe$(bipy)_3^{2+}$ and Ru$(bipy)_3^{2+}$ (bipy – bipyridine) as a catalyst in place of cerium, the $HBrO_2$-based autocatalytic core remains intact.[49,50]

Some oxidation reactions by nitric acid are autocatalytic. Epstein studied the kinetics of the oxidation of Fe^{2+} oxidation. He suggested that two active species are responsible for the amplification, HNO_2 and NO.[51] Similarly, the salts of Fe$(phen)_3^{2+}$ (phen - phenanthroline) or the Fe$(bipy)_3^{2+}$ cations can react autocatalytically with nitric acid.[52] HNO_2 is also an autocatalyst in bromide oxidation by nitrate. In this reaction, $BrNO$ is an initial product of the oxidation of Br^- by HNO_2. NO_2, which is a product of the reaction of nitrate with nitrite, oxidizes nitrosyl bromide to the highly active $BrNO_2$ and releases NO. More HNO_2 comes from the synproportionation of NO and NO_2.[49] The arsenite,[51] thiocyanate,[48] and hydroxylamine[50] oxidations by nitric acid proceed via a similar autocatalytic pathway. For details of these reactions, we refer the reader to the excellent review by Bazsa and Epstein.[57]

The autocatalytic chlorite-bromide reaction [Eq. (21)] has a mechanism that is similar to the mechanism of the autocatalytic core in the Belousov-Zhabotinski reaction.
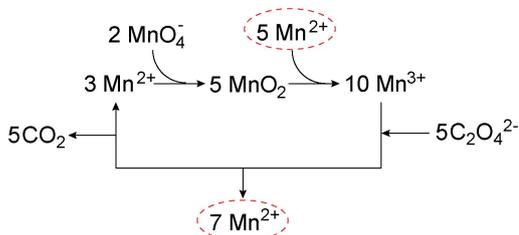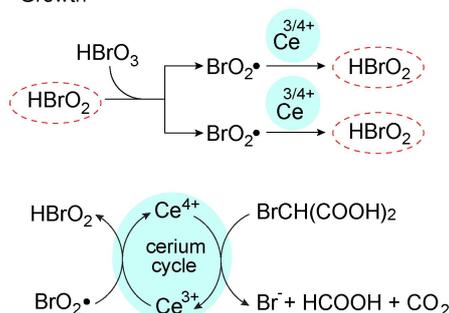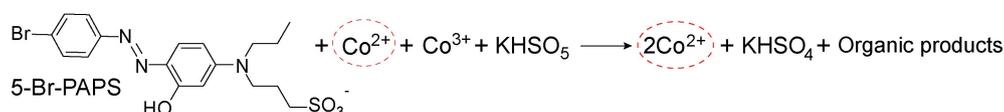
Figure 7. Featured inorganic autocatalytic reactions. a) Simplified mechanism for Mn^{3+} and Mn^{2+} amplification in the permanganate-oxalate reaction.[19b] b) Representation of an autocatalytic reaction sequence in a Belousov-Zhabotinky reaction.[9] c) Autocatalytic Co^{3+} oxidation of 2-(5-Bromo-2-pyridylazo)-5[N-n-propyl-N-(3-sulfopropyl)amino]phenol (5-Br-PAPS).[48]

$$ClO_2^- + 4H^+ + 4Br^- \rightarrow Cl^- + 2Br_2 + 2H_2O \qquad (21)$$

The reaction is autocatalytic on Br_2. Simoyi suggested[58] that Br_2 is a catalyst for the oxidation of bromide by chlorite. In the proposed catalytic cycle, Br_2 disproportionate in water into HOBr and Br^-. HOBr reacts with $HClO_2$, producing $HBrO_2$ and HOCl, both of which react with bromide, producing two molecules of Br_2. Therefore, this cycle generates two molecules of Br_2 from one.

Similarly, iodine can react with chlorite autocatalytically, forming an ICl intermediate.[59] Figlar and Stanbury found an autocatalytic reaction between SCN^- and ClO_2. It proceeds via the autocatalytic formation of $(SCN)_2$ and $(SCN)_2^-$, which gives rise to other reactive species.[60] Epstein and co-workers reported the autocatalytic oxidation of thiourea by Br_2, with the formation of urea, bromide, and sulfate.[61]

The nitrosylation of thiourea disulfide has a sigmoidal kinetic profile. Nitrogen, cyanide, sulfate, and thiocyanate (SCN^-) are the products of this reaction. SCN^- acts as an autocatalyst. It reacts with HNO_2, affording NOSCN, which is a powerful nitrosylating agent.[62]

Oxidation reactions by Co(III) form another class of autocatalytic reactions. The oxidation of hydrazine by carbonatocobaltate(III) is the first example. The mechanism underlying this reaction involves an alleviated electron transfer between carbonatocobaltate(III) and cobalt(II) hydrazine complexes. The authors assumed that the Co(II) species facilitates the reduction of carbonatocobaltate (III) in the process similar to the reaction between the Co(II)-hydrazine complex and Cu (II), which releases N_2H_2.[63] The reaction between 5-Br-PAPS dye

with Co^{3+} and Co^{2+} in the presence of Oxone ($KHSO_5$) (see Figure 7(c)) is autocatalytic (Figure 8).[48] Like in the previous case, Co^{2+} serves as an autocatalyst in the system. Running this
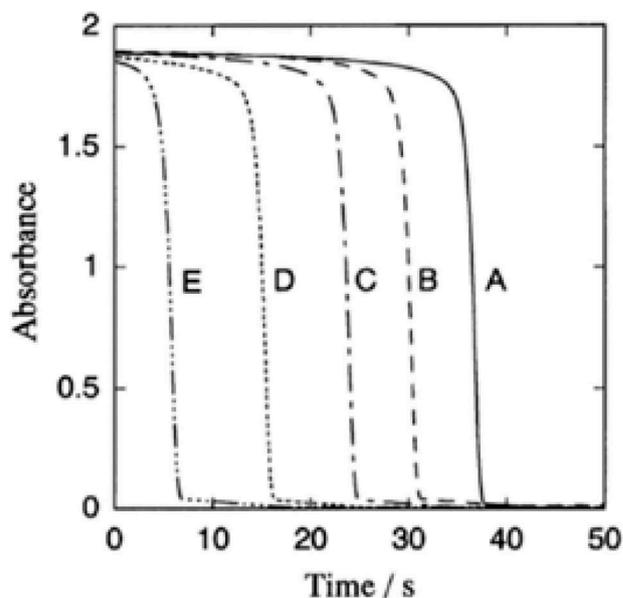
Figure 8. Autocatalytic curves for the reaction of 5-Br-PAPS with Co^{3+} and Co^{2+}. A) [Co(II)] = 0, B) [Co(II)] = $1.5*10^{-8}$ M, C) [Co(II)] = $3*10^{-8}$ M, D) [Co(II)] = $7.5*10^{-8}$ M, E) [Co(II)] = $1.5*10^{-7}$ M[48] Reproduced from Ref. [48] with permission. Copyright 1998 Elsevier.

reaction in microdroplets in microfluidics enabled the visualization of the sigmoidal autocatalytic kinetics.[64]

The copper(II)-catalyzed oxidation of β-alanine is another example of metal-based autocatalytic inorganic reactions. In this reaction, 3-oxopropanoic acid forms a stable peroxide complex with copper, which enables the further oxidation of β-alanine.[70] A similar chain mechanism was observed in the oxidation of nitrobenzene by iron (III), where quinone-like species amplify the rate of the formation of the Fe(II) species.[69]

Another prominent example of inorganic autocatalysis is the release of hydrogen from ammonia borane. NH_2BH_2 was assigned as an autocatalyst in this reaction, based on our computational studies. The process responsible for the emergence of autocatalysis in this system is the direct reaction between ammonia borane and NH_2BH_2 with the formation of a dimer that can dissociate with the formation of two equivalents of NH_2BH_2 along with the release of hydrogen. Two NH_2BH_2 molecules form a four-membered cyclic dimer. The linear dimer of NH_2BH_2 can react with one more equivalent of NH_2BH_2, affording a six-membered cycle.[66]

Reactions generating metal nanoclusters and nanoparticles form a large class of autocatalytic reactions. One of the oldest autocatalytic reactions is the decomposition of silver oxide at 250 °C, where silver is the autocatalyst.[67] Reduction of H_2PtCl_6 on Al_2O_3 is also autoamplified because the kinetics of nucleation and growth is sigmoidal.[65] A similar autocatalytic process is the formation of polyoxoanion-stabilized iridium nanoclusters via the reduction of $[(1,5\text{-}COD)Ir*P_2W_{15}Nb_3O_{62}]^{8-}$ with hydrogen.[68] Mo_{36} nanoclusters are formed from Na_2MoO_4 autocatalytically. The autocatalysis can be explained by the nanocluster seeding in the early stages of the reaction. Miras et al. constructed different auto- and cross-catalytic cycles that form molybdenum nanoclusters with different compositions.[72] Autocatalytic kinetics seems to be a general trend in reactions involving the reduction of metals to their metallic form. Reduction of silver halides in photographic processes and reduction of nickel salts during electroless plating are representative examples.[3,4]

The reaction of NO and CO on a Pt(100) surface at low concentrations of adsorbates also proved to be autocatalytic. The mechanism underlying this autocatalysis involves attractive interactions between adsorbed products and reagents on the catalyst.[73]

A distinctive future of inorganic autocatalytic systems is that they often develop bistable and oscillatory behaviors with the addition of some reactants or under special conditions.[11,9,74,75] No other class of autocatalytic reactions is capable of an as broad range of dynamic behaviors as inorganic (mostly redox) reactions. This uniqueness is attributed to the mechanistic complexity of these reactions that makes them behave as cubic autocatalysis and to the fact that unstable autocatalysts (e.g. $HBrO_2$) are often destroyed in some coupled reactions.[11,76]

In summary, inorganic autocatalytic reactions have an advantage of their high rates and high nonlinearity, but because of the complexity of their mechanism and difficulty in modifying the molecular structures of the starting materials, they are not a primary target for developing new autocatalytic systems. Thus, in the next section, we will discuss autocatalytic

systems based on organic molecules, which have a great diversity of molecular structures that can be designed and synthesized.

4. Autocatalysis Based on Organic Chemistry (Excluding Template-Assisted Reactions)

The essential organic autocatalytic reactions that are not based on the template effect are summarized in Table 2.

4.1. Acid/Base Autocatalysis

Acid and base autocatalytic reactions were reviewed by Ichimura;[77] therefore, we will only focus on the representative examples for this class of reactions. Acid autocatalysis is among the mechanistically simplest and most widespread forms of autocatalysis. It is the basis of chemically amplified photoresists; thus, its importance goes beyond academic interest[78] In acid autocatalysis, the reaction that forms acid is also catalyzed by acid. There are a few general strategies to design acid autocatalysis.

The first strategy is to use acidic ester hydrolysis. Esters are not acidic or basic by themselves, but their hydrolysis is catalyzed by acids and produces acid. The efficiency of autocatalysis will largely depend on two factors: the susceptibility of a particular ester to acid catalysis and the strength of the resulting acid. Xu et al. studied the hydrolysis of methyl oxalate and showed that the reaction proceeds in two stages: both stages are autocatalytic on H_3O^+ (Figure 9a).[79] The reaction takes about an hour for completion at 75 °C. Generally, autocatalysis in the hydrolysis of methyl esters is inefficient. However, the efficiency increases significantly with the use of tert-butyl esters because they hydrolyze through the S_N1 mechanism, which is more sensitive to acid catalysis than the S_N2 mechanism; this characterizes the hydrolysis of methyl esters. Tert-butyl esters and even phenol ethers are common elements of chemically amplified photoresists.[78c,80,78b]

The second strategy is to use sulfonic esters. Sulfonic acids are much stronger than carboxylic acids. Their high acidity makes them efficient catalysts and increases the efficiency of the autocatalysis; however, simple sulfonic esters are insusceptible to acid catalysis. Ichimura and others developed several tricks to overcome this insusceptibility. p-tert-butyl carbonates of benzyl sulfonates hydrolyze through a two-stage process where the first stage is the acid-catalyzed hydrolysis of a tert-butyl carbonate, which is highly susceptible to acids, whereas the second stage is the fast rearrangement of p-hydroxy-benzyl sulfonate to p-quinomethane and sulfonic acid.[78c] The use of sulfonyl esters derived from trioxane is another elegant approach (Figure 9b). The acid-catalyzed hydrolysis of the trioxane ring produces sulfonyl esters of β-hydroxypropanal, which decomposes, forming a sulfonic acid and acrolein.[81] Brainard et al. used γ-hydroxy sulfonic esters. These molecules

ChemSystemsChem

Reviews
doi.org/10.1002/syst.202000026

Chemistry Europe
European Chemical
Societies Publishing

Table 2. Essential non-template organic autocatalytic reactions.
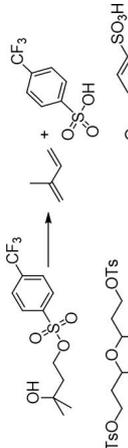
Reaction	Autocatalyst	Mechanism	$k_{autocat}$	k_{noncat}	Ref.
	Sulfonic acid	Acidic	$48*10^3$ s^{-1}, 100 °C	33.8 M*s^{-1} 100 °C	[82]
	Sulfonic acid	Acidic			[81]
$(COOCH_3)_2 + 2H_2O \rightleftharpoons (COOH)_2 + 2CH_3OH$	Oxalic acid	Acidic			[79]
+ HCl	HCl	Acidic	$k = 0.0058$ M^{-2} min^{-1}		[108]
Figure 10(c) on Base autocatalysis	Amine base	Basic			[109]
	Heterocyclic base	Basic	16.6 M^{-2} h^{-1}	0.0614 M^{-1}*h^{-1}	[86]
Figure 20 Mutarotation of Glucose	Photo-catalyst Glucose	Photo-catalysis Acid-base			[110a] [111]
	Alkoxide adduct	Nucleophilic	0.21 M^{-2} s^{-1}	0.06 M^{-1} s^{-1}	[112]
+ N$_2$	Benzen-sulfonic acid	Radical-based			[113]
	SmI$_3$	Lewis acid-based			[114]
2 + I$_2$ + CH$_3$CO$_2$H $\longrightarrow$	Iodoso compounds	Electon-transfer based			[115]
2 + H$_2$O + CH$_3$CO$_2$H	Ureatane	Lewis acid-based			[116]
R=Me, Bu, i-Pr, CH$_3$OCH$_2$CH$_2$, HOCH$_2$CH$_2$ Figure 13	Thiols	Nucleophilic branched-chain reaction	0.25 s^{-1} M^{-1}†	$7*10^{-5}$ s^{-1}†	[22]
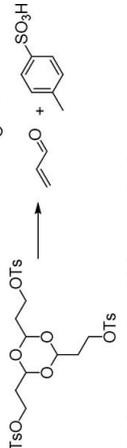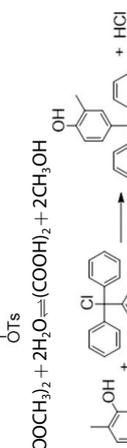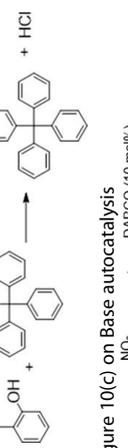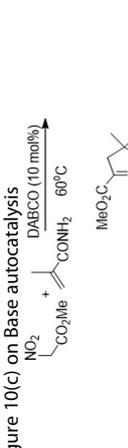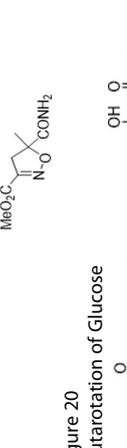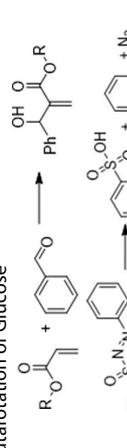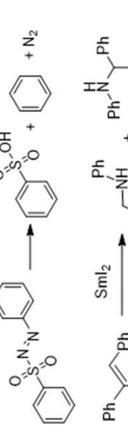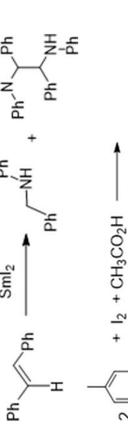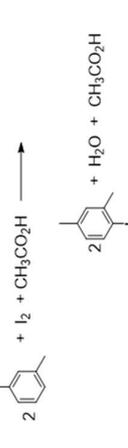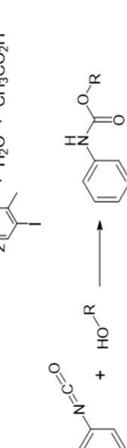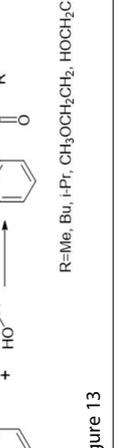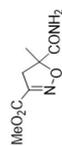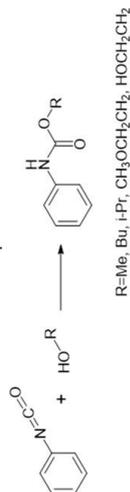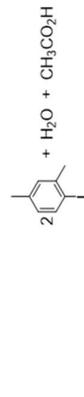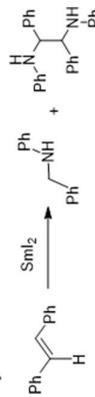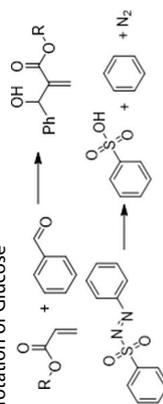
Table 2. continued

Reaction	Autocatalyst	Mechanism	$k_{autocat}$	k_{noncat}	Ref.
	F⁻	Nucleophilic branched-chain reaction			[91]
Decomposition of the compound in Figure 15	H₂O₂	Branched-chain reaction			[93]
Formose reaction	Glycoaldehyde	Nucleophilic			[8c, 20, 117]
Figure (16(a))	Cu-ligand complex	Ligand induced catalysis	$0.13\ \mathrm{s^{-1}\,M^{-3}}$†	$1.1*10^{-7}\ \mathrm{s^{-1}\,M^{-2}}$†	[23]
	$(P^tBu_3)_2Pd(H)(Br$	Activation of LDA by product	$(1.5\pm0.3)\times10^{-4}$	$(1.3\pm0.4)\times10^{-6}$	[105]
		Induction of oxidative addition by a product	$0.00987\ \mathrm{M^{-1}\,s^{-1}}$†		[106]
Figure 18		Hydrogen activation by product	$125.95\ \mathrm{M^{-1}\,s^{-1}}$	$0.09\ \mathrm{s^{-1}}$	[107]
Figure 19	Pt colloids	heterogeneous	(Vacuum Sealed) $31.92\ \mathrm{mM^{-2}\,min^{-1}}$†	$0.014\ \mathrm{mmole^{-1}\,l^1\,min^{-1}}$†	[118]
	HOAc	Acidic			[119]
	Product-zinc complex	Activation of aldehyde by zinc complex of the alcohol product			[120]
Figure 20 (a)	Product-zinc complex	Activation of aldehyde by zinc complex of the alcohol product			[121]
Figure 14	Thiols	Nucleophilic branched-chain reaction			[89]
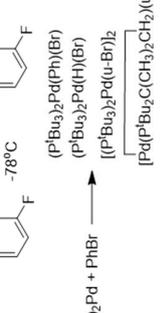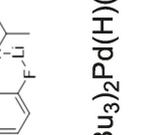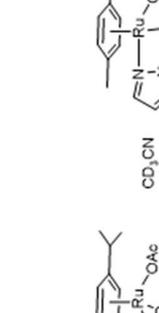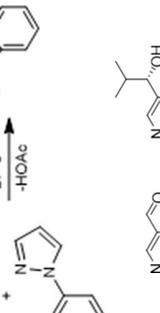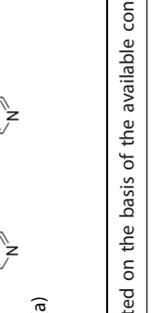
† – Calculated on the basis of the available concentration data. These data were fitted to the rate equation $r = k_{autocat}[S_1]..[S_n][P] + k_{noncat}[S_1]..[S_n]$, where Sn are the reaction substrates and P is the product.

ChemSystemsChem

Reviews
doi.org/10.1002/syst.202000026

**Chemistry
Europe**
European Chemical
Societies Publishing
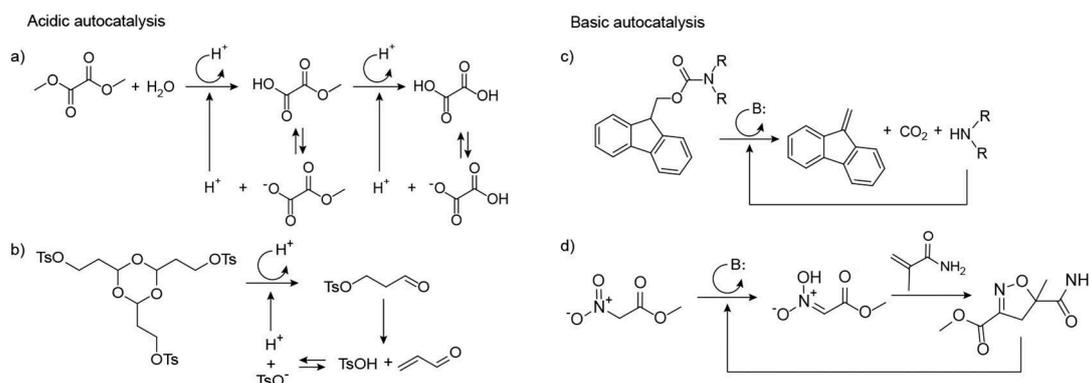
Figure 9. Examples of acidic and basic autocatalysis. a) Autocatalytic dimethyloxalate hydrolysis.[79] b) Autocatalytic decomposition of 2,4,6-tris[2-(p toluenesulfonyloxy)ethyl]-1,3,5-trioxane.[81] c) The autocatalytic fragmentation of N-substituted 9-fluorenylmethyl carbamates. The substituents include piperidine, cyclohexylamine, diethylamine, dicyclohexylamine, and cis-dimethylpiperidine.[84] d) The autocatalytic [2 + 3] cycloaddition of methyl-2-nitroacetate with methacrylamide.[86]

hydrolyze through the SN1 mechanism by protonation of the γ-hydroxyl and the subsequent formation of a carbocation[82,83]

Base autocatalysis is rarer than acid autocatalysis. Fmoc (Fluorenylmethyloxycarbonyl) deprotection is the best-documented example of base autocatalysis. Ichimura showed that the secondary amine (e.g., piperidine) released during deprotection catalyzes further deprotection of this amine with the release of dibenzofulvene and carbon dioxide (Figure 9(c)). This autocatalysis is slow, taking about two hours for completeness at 100 °C in dioxane.[84] It was applied to design a positive photoresist based on siloxane resins.[85] Guideri et al. reported autocatalysis in the cycloaddition of derivatives of nitroacetic acid to acrylamide (Figure 9(d))[86] Although the source of the autocatalysis was not completely proved, it is likely to have come from the basic properties of the isoxazole derivatives formed in this reaction.

The formaldehyde-sulfite autocatalytic reaction is an interesting example of base autocatalysis with hydroxyl as the autocatalyst. This reaction occurs in a mixture of aqueous solutions of formaldehyde and sodium sulfite (Figure 10). Importantly, the percentage of formaldehyde is 99% in the hydrated dihydroxymethylene form in solution, whereas only dehydrated aldehyde reacts with sulfite. The conversion of dihydroxymethylene to the aldehyde is catalyzed by hydroxyls. The addition of sulfite dianion to formaldehyde generates the alcoholate anion, which is a strong base, generating hydroxyls in its reaction with water. Therefore, the addition of sulfite to formaldehyde generates hydroxyls that catalyze the formation of formaldehyde from dihydroxymethylene, creating an autocatalytic loop.[24,87] Once initiated, the formaldehyde-sulfite reaction is fast, taking only seconds to complete.

4.2. Autocatalytic Organic Reaction Networks

Boutlerow discovered the formose reaction in 1861.[8c] It is the first discovered autocatalytic reaction network and the first reaction with clear prebiotic relevance. According to Breslow,
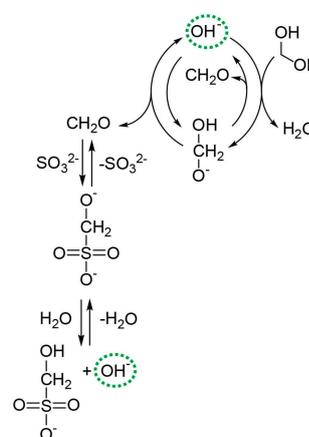
Figure 10. The possible mechanism underlying the formaldehyde–sulfite reaction.[24,87]

glycolaldehyde is the autocatalyst in this reaction (Figure 11).[20] Initially, it forms in minute amounts by the condensation of two molecules of formaldehyde through an unknown and inefficient mechanism. Once formed, glycolaldehyde undergoes a sequence of transformations consisting of five major reactions: (i) aldol condensation with formaldehyde; (ii) the isomerization of an aldehyde to a ketone; (iii) a second aldol condensation with formaldehyde; (iv) the isomerization of a ketone to an aldehyde; and (v) an retro-aldol reaction that produces two molecules of glycoaldehyde. The last step is the source of exponential growth. In addition to the products mentioned in this scheme, the reaction produces.

Semenov et al. showed that the reaction between the thioesters of amino acids and cystamine in phosphate buffer is autocatalytic.[22,88] This reaction is a good example of an autocatalytic network. It does not involve catalysis in a "classic" sense and the intermediates of this reaction are stable, separable compounds. In addition, it exhibits very clean sigmoidal kinetics (Figure 12).

ChemSystemsChem

Reviews
doi.org/10.1002/syst.202000026

**Chemistry
Europe**
European Chemical
Societies Publishing
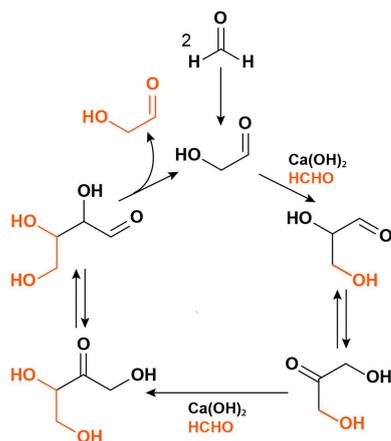
Figure 11. Formose reaction. Formaldehyde, at the top of the scheme, dimerizes to glycolaldehyde. In the presence of calcium hydroxide, glycolaldehyde reacts with two equivalents of formaldehyde in the aldol reaction. Then the product undergoes a rearrangement to form the aldehyde, which produces two equivalents of glycoladehyde in a retro-Aldol reaction.[20]
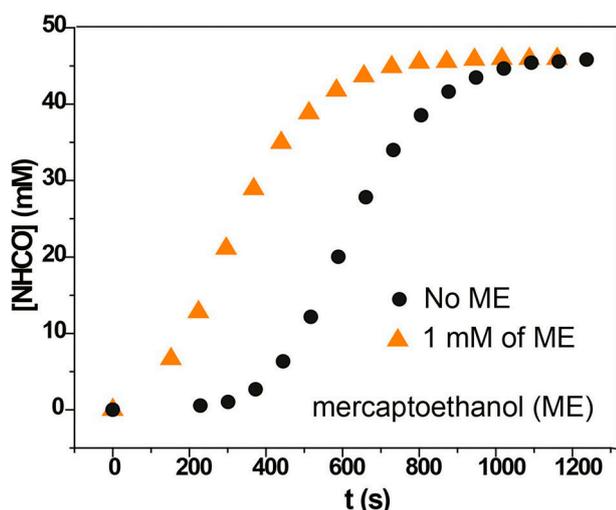
Figure 12. A graph showing sigmoidal kinetics and the elimination of the lag period by the addition of β-mercaptoethanol (ME) in the reaction between L-alanine ethyl thioester (46 mM) and cystamine (46 mM). NHCO denotes the total concentration of amides, which was measured by 1H NMR spectroscopy. The reaction was carried out in phosphate buffered at pH 7.5.[22] Copyright 2016 Springer Nature.

Figure 13 shows the mechanism of amplification in the reaction between L-alanine ethyl thioester and cystamine. It involves two steps: (i) cysteamine (CSH) rapidly reacts with thioester through native chemical ligation (NCL), yielding two thiols: ethanethiol and alanine 2-mercaptoethylamide; (ii) these two thiols undergo a thiolate-disulfide exchange with a cystamine, yielding two molecules of cysteamine. Because one molecule of cysteamine generates two molecules of cysteamine, this network proceeds autocatalytically. Semenov and co-workers used this reaction to design bistable and oscillatory reaction networks in a flow reactor.[22]

The design strategy behind this autocatalytic system was the search for reaction networks with a branched structure. Kinetic data showed that the formation of amides from thioesters of amino acids by the direct attack by an amine group is orders of magnitude slower than the formation of amides by NCL at neutral pH. Combination of these kinetic data with the knowledge that NCL produces two thiol molecules from one and that thiols undergo fast thiol-disulfide exchange generated the proposal of the reaction network shown in Figure 13.

Sun and Anslyn published an alternative thiol autocatalytic network[89] (Figure 14). They used a di-mercaptomethyl derivative of Meldrum's acid that reacts with mercaptoethanol, releasing two molecules of methyl mercaptan. When the derivative of Meldrum's acid is mixed with a disulfide of mercaptoethanol, these two molecules of methyl mercaptan produce two molecules of mercaptoethanol via disulfide exchange. Therefore, one molecule of mercaptoethanol produces two molecules of mercaptoethanol. Although Sun and Anslyn call their system auto-inductive, this system is autocatalytically closed (see the kinetics chapter). It represents a typical autocatalytic reaction network.

Another class of autocatalytic reactions is based on the para-substituted benzyl alcohols and their analogs.[90,91,92] Phenolates of para-hydroxy benzyl alcohol derivatives are unstable towards rearrangement into 4-methylene-2,5-cyclohexadien-1-one. Shabat was the first to use this rearrangement for auto-amplification.[93,94] His group developed a chain reaction that autocatalytically produces p-nitroaniline and hydrogen peroxide from the specially designed substrate (Figure 15) and oxygen in the presence of choline oxidase. The substrate consists of four parts: (i) phenylboronic acid, (ii) two choline groups, (iii) p-nitroaniline, and (iv) a central fragment that connects all parts. The autocatalytic process is initiated by small amounts of hydrogen peroxide that converts the phenylboronic acid derivative to the phenol derivative, which decomposes to 4-methylene-2,5-cyclohexadien-1-one and exposes the phenol group of the central fragment. This fragment undergoes a triple rearrangement, releasing p-nitroaniline and two molecules of choline. Oxidation of choline by oxygen in the presence of choline oxidase releases two molecules of hydrogen peroxide that react with two boronic acids and activate two substrate molecules. Therefore, it becomes a chain reaction. We notice that this reaction network is not autocatalytically closed because it requires a catalyst (choline oxidase) which is not a part of the chain process.

Baker and Phillips used a similar principle to amplify exponentially the concentration of fluoride anions by derivatives of para-difluoromethylaniline.[91] For a comprehensive overview of this type of autocatalytic reaction, we refer the reader to excellent reviews by Shabat and Prins.[95,96] As in the case of thiol-based autocatalytic networks, the design of autocatalytic networks with derivatives of para-hydroxy benzyl alcohol uses the idea of the branched-chain reaction.

Copper-catalyzed azide-alkyne cycloaddition (CuAAC) is a key element in several autocatalytic systems. Finn and Fokin first noticed that reactions of tripropargylamine with various

ChemSystemsChem

Reviews
doi.org/10.1002/syst.202000026

Chemistry Europe
European Chemical
Societies Publishing

azides are autocatalytic. They attributed this autocatalysis to stability and the catalytic properties of the complexes of Cu(I) with tris-triazole formed in this reaction.[97,98] Copper-catalyzed azide-alkyne cycloaddition is a fast reaction, even without tris-triazolyl ligands; thus, the contribution of non-autocatalytic pathway was probably significant in the first autocatalytic CuAAC. Semenov et al. eliminated the effect of the non-autocatalytic pathway by using Cu (II) salts as a starting material (Figure 16(a)).[23] In this system, the tris-triazolyl product catalyzes the reduction of Cu(II) to Cu(I) and stabilized Cu(I). Therefore, the tris-triazolyl product catalyzes the formation of Cu(I) complexes that are the catalysts for its formation from the inert precursor (i.e., Cu(II) salt). This cooperation between the reduction of copper as well as the cycloaddition provides more than a 400-fold time difference in the background reaction rates for the non-catalytic and autocatalytic pathways. This low rate of background reaction allows the observation of an autocatalytic front in this reaction (Figure 16b). The groups of Devaraj and Fletcher used CuAAC combined with the formation of micelles, vesicles, and spherical nanostructures (Figure 16c). Devaraj and co-workers demonstrated the self-replication of vesicles from fatty azides and tripropargylamine.[99] He also showed a very clean sigmoidal growth of nanospheres from azide-functionalized tripeptides and tripropargylamine.[100] Fletcher and co-workers showed self-reproducing micelles from maltose azide and alkyl-substituted acetylenes and studied the factors that influence their growth.[101] Binder and co-authors observed autocatalysis in a CuAAC-based polymerization reaction.[102]

Both thiol and CuAAC autocatalytic systems are attractive platforms for the development of functional systems because of the accessibility of structural modifications of their components. Nevertheless, the thiol system has the advantage of a clear mechanistic understanding of the reactions involved. This understanding provides good control over the kinetics of the thiol-based reaction networks. On the other side, the CuAAC
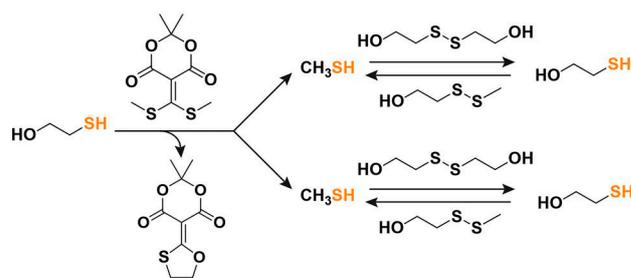
Figure 14. Mechanism underlying the autocatalytic reaction between a di-mercaptomethyl derivative of Meldrum's acid and a disulfide of mercaptoethanol.[89]
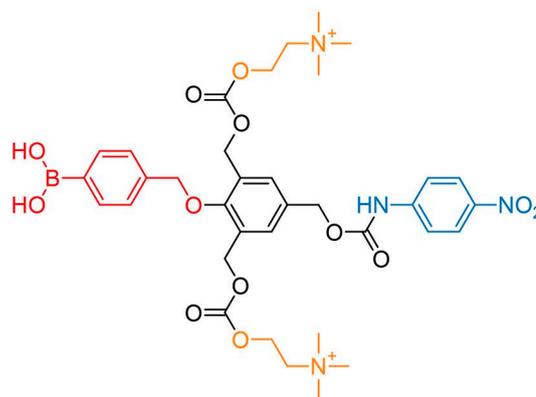
Figure 15. The structure of the substrate used by Shabat et al. to amplify the concentration of hydrogen peroxide.[93,94]

systems have an advantage of high orthogonality of their core chemistry while thiols, which are strong nucleophiles, react with a broad range of electrophilic and oxidizing compounds.
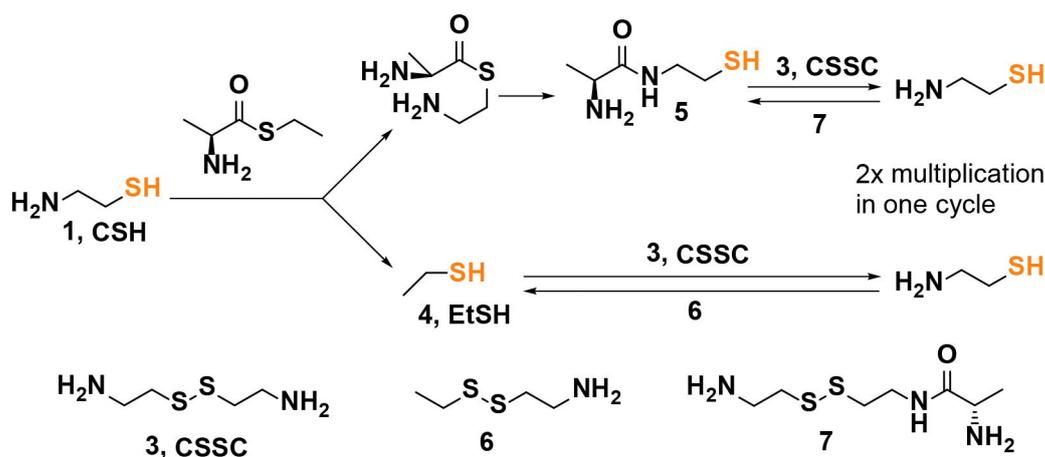
Figure 13. Mechanism underlying the autocatalytic reaction between L-alanine ethyl thioester and cystamine. In this scheme, cysteamine reacts with L-alanine ethyl thioester, forming cysteamine thioester. Thioester rearranges to form amide, which can exchange with cystamine, releasing cysteamine. Concomitantly, ethanethiol from the first reaction is also exchanged with cystamine, producing another equivalent of cysteamine. Cysteamine is duplicated in each cycle.[22] Reproduced with permission from Ref. [22]. Copyright 2016 Springer Nature.

ChemSystemsChem

Reviews
doi.org/10.1002/syst.202000026

Chemistry Europe
European Chemical
Societies Publishing
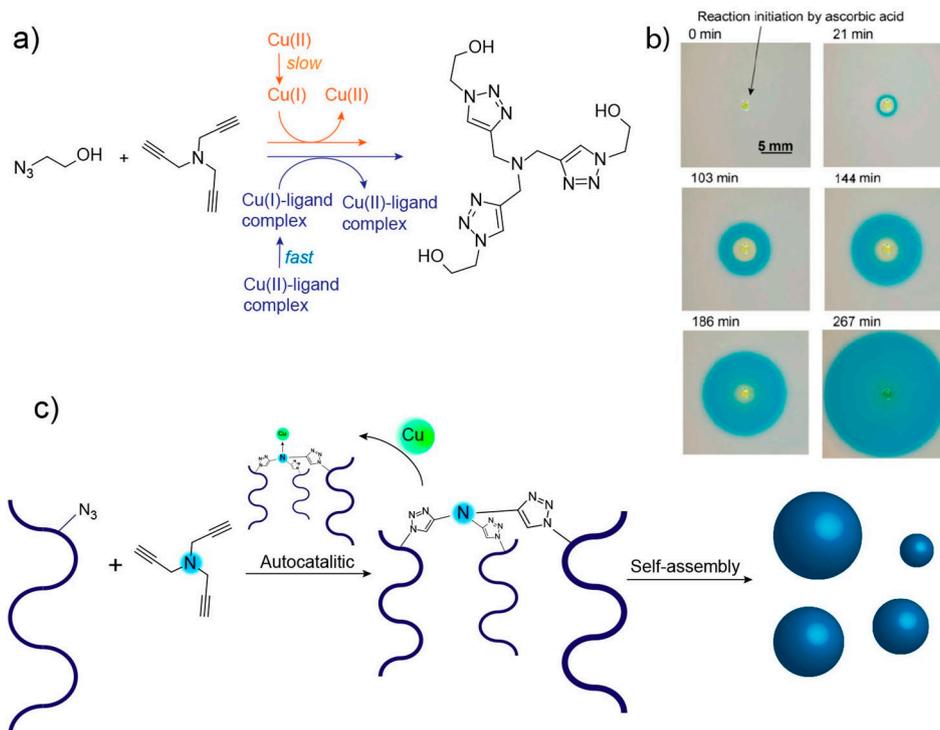
Figure 16. Autocatalytic "click"-reactions. a) The autocatalytic formation of tris(3-hydroxypropyltriazolylmethyl)amine in the presence of Cu(II) salts.[23] b) Autocatalytic front propelled by the reaction shown in panel (a). The blue comes from the Cu(II) complex of tris(3-hydroxypropyltriazolylmethyl)amine. c) Schematic representation of an autocatalytic formation of tris-triazole peptides, which can self-assemble into the nanospheres.[100] Reproduced with permission from Ref. [23] with permission. Copyright 2018 American Chemical Society.

4.3. Organometallic Autocatalysis

Autocatalysis in organometallic reactions remains a rare phenomenon. The lithiation of 3-fluorophenyl diisopropylcarbamate with lithium diisopropylamide (LDA) shows autocatalytic kinetics (Figure 17).[103] Collumn and co-workers suggested that when the LDA dimer reacts with the starting compound, it forms a bicyclic intermediate with two lithium atoms. This intermediate is a more efficient lithiation agent than LDA dimer itself; thus it acts as an autocatalyst. The same group later discovered similar behavior during the lithiation of 1-chloro-3-(trifluoromethyl)benzene[104] and 2-fluoropyridines[105] with LDAs.

Surprisingly, the oxidative addition of PhBr to $Pd(PBu^t_3)_2$ is an autocatalytic reaction. The thermal decomposition of an oxidative addition product generates phosphonium salt and $Pd(PBu^t_3)_2(H)(Br)$, which initiate the autocatalytic cycle. In solution, the ligand can form the phosphonium salt PBu^t_3*HBr, which can then transfer HBr to the Pd metal center, forming hydridobromide $Pd(PBu^t_3)_2(H)(Br)$. This complex can exchange with PhBr, affording the final oxidative addition product $Pd(PBu^t_3)_2(Ph)(Br)$. The last reaction occurs faster than the direct oxidative addition of PhBr. The mechanism underlying this exchange involves the formation of ionic species $[HPBu^t_3][Pd(PBu^t_3)(Br)]$. Pd(0) here can easily react with PhBr.[106]

Another autocatalytic reaction is the ruthenium-catalyzed hydrogenation of acetophenone[93] (Figure 18). In the initial step of this reaction, dihydrogen attaches to the initial ruthenium-hydride complex. Then, 1-phenylethan-1-ol, which is the final product of hydrogenation, assists in the heterogeneous cleavage of the H—H bond in the ruthenium dihydrogen complex. The formed ruthenium dihydride complex reduces acetophenone to 1-phenylethan-1-ol, closing the autocatalytic cycle.

Ruthenium-catalyzed C—H activation in 2-phenylpyridine,[122] 1-phenyl-1H-pyrazole, and 2-phenyl-4,5-dihydrooxazole[119] behave autocatalytically. The initial catalyst, $[Ru(OAc)_2(p-cymene)]$, forms the cyclometallation adduct upon the insertion of C—H. This process releases acetic acid, which initiates further removal of acetate from the original catalyst structure. Thus, acetic acid is an autocatalyst.

Figure 17. Autocatalytic lithiation of 3-fluorophenyl diisopropylcarbamate with LDA.[103]

ChemSystemsChem

Reviews
doi.org/10.1002/syst.202000026

**Chemistry
Europe**
European Chemical
Societies Publishing
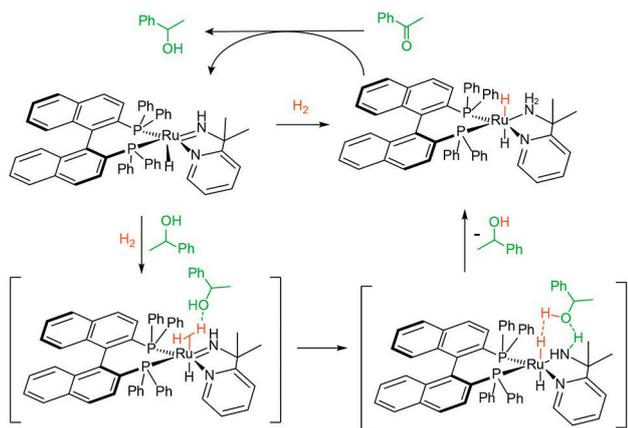
Figure 18. Ru-catalyzed hydrogenation of acetophenone.[107]

The four-membered platinacycle (Figure 19) with naphthalene and the six-membered cycle with triphenylene react autocatalytically with diphenylacetylene, forming a cyclo-addition product. The byproduct of this reaction, Pt-alkyne complex, reacts with oxygen, and produces Pt metal. Authors suggest that Pt colloids act as a heterogeneous autocatalyst in these reactions.[118]

The rhodium-catalyzed dehydrogenation of $H_3B–NMe_2H$ to cyclic $(H_2B–NMe_2)_2$ is another example of a transition-metal-based autocatalytic reaction. The mechanism underlying this reaction involves multiple intermediates and was discussed in detail by Sewell et al.[123] Despite the opportunity to design organometallic autocatalytic reactions based on the formation of catalytically active ligands, all reactions that we discussed in this section are the result of serendipitous discoveries.

4.4. Chiral Autocatalysis

The homochirality of biological molecules is one of the greatest mysteries of life. Most likely, homochirality has its roots in the very early stages of the emergence of life, where an incidental excess of one of the isomers was amplified in some kind of autocatalytic process. As Blackmond pointed out,[124] a simple exponential autocatalysis is insufficient to amplify a small enantiomeric excess of a product because enantiomeric tran-sition states will have an identical energy state, resulting in

identical autocatalytic rate constants. There are at least two ways to overcome this obstacle. The first solution is a Frank model where two enantiomers of the product are mutually antagonistic.[125] The second possibility is the involvement of more than one product molecule in the transition state, resulting in cubic autocatalysis and hyperbolic growth that can amplify initial excess of one of the isomers even when rate constants are identical. Perhaps these strict mechanistic demands are the reason for the rarity of enantiomeric autocatalysis. With many excellent reviews available,[12h–j,l–n] we will only discuss its experimental examples briefly.

Among the earliest examples is the addition of Et_2Zn to benzaldehyde.[126] A catalytic amount of $TiCl_4$ coordinates the alcohol product and the aldehyde, favoring the anti-orientation of the benzene rings in the homochiral transition state. After a workup, Alberts and Wynberg obtained a 32% enantiomeric excess (ee) of the product.

The exploration of zinc-organic addition reactions inspired the Soai group to discover the most efficient asymmetric autocatalytic system. In studying the addition of diethylzinc to pyridine-3-carbaldehyde, this group found that the reaction is significantly faster than the addition to benzaldehyde.[127] Shortly afterwards, they established the autocatalytic addition of diisopropylzinc to pyridine-3-carbaldehyde, which produced 35% ee.[128] The substitution of pyridine for pyrimidine generated a very efficient autocatalytic system.[120] This design eliminated the disruption of autocatalysis by the non-active rotational isomer of pyridine-3-carbaldehyde. Even when in the initial mixture, the alcohol was in 5% ee; this was enough to achieve 55% ee in a single round of the reaction. As a further improvement, 2-alkynyl-5-pyrimidyl alcohols displayed up to 10^7 amplification factor (see Figure 20).[121]

The combination of crystallographic[129] and computational studies[130] suggests the formation of a 12-membered cycle in the transition state that defines the stereochemistry of the

Figure 19. A) Autocatalytic cycloaddition of diphenylacetylene to a cyclo-platinated naphthalene. B) The autocatalytic curves of the reaction (a). Blue dots denote the vacuum-sealed reactor; green triangles denote the N_2 atmosphere; red squares denote the presence of O_2[118] Reproduced with permission from Ref. [118]. Copyright 2005 American Chemical Society.
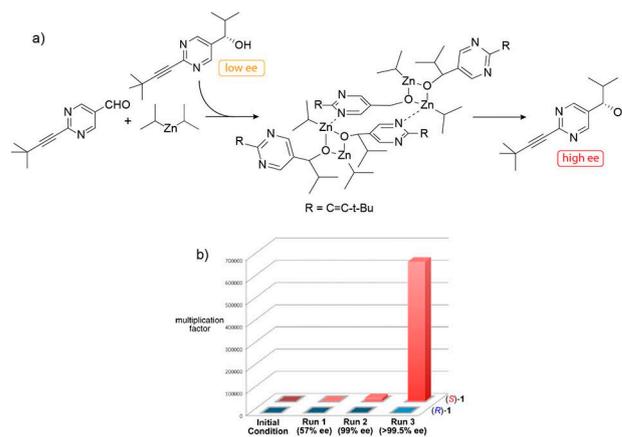
Figure 20. Soai reaction. A) The addition of diisopropyl zinc to 2-(*tert*-butylethynyl)pyrimidine-5-carbaldehyde autocatalytically forms the chiral alcohol. The reaction proceeds through the 12-membered cyclic transitional state that defines the enantioselectivity. A small enantiomeric excess of the product is amplified in the reaction. B) The amplification of a single enantiomer of the product in reaction (a).[121,129,12l] Reproduced with permission from Ref. [121]. Copyright 1999 Wiley-VCH.

ChemSystemsChem

Reviews
doi.org/10.1002/syst.202000026

Chemistry Europe
European Chemical
Societies Publishing

product. The stereochemical induction may occur without an initial addition of the product. For instance, Soai and Shibata mediated the photoequillibrium shift in chiral olefins by using circularly polarized light to start the autocatalysis.[131] Chiral crystals, made from achiral compounds, also successfully initialized the amplification. Even $^{13}C/^{12}C$ and $^{14}N/^{15}N$ isotopic enantiomers can trigger an asymmetric autocatalysis.[132]

Several systems with similar additions of the zinc-organic compounds display amplification as well. Careira and co-workers used catalytic amounts of the enantiopure product in the $ZnEt_2$-mediated addition of alkyne to a ketone in the synthesis of the antiretroviral drug, Efavirenz (Figure 21).[133]

Later, Espinet proved the chiral autoamplification by the addition of $ZnEt_2$ to $PhC(O)CF_3$.[134] Oligomeric zinc-containing cycles are responsible for the enantiomeric induction in these systems. The chiral alcohol product coordinates to zinc in cycles and introduces a stereochemical bias, which favors the formation of its replica.

The examples of asymmetric amplification are not limited to the chemistry of zinc. Furrer and co-workers investigated the stereochemistry of the reduction of two camphor enantiomers by potassium in liquid ammonia.[135] The reaction revealed asymmetric autocatalysis. Ketyls appear in the first step of the reaction and then undergo a disproportionation reaction via H-transfer. This transfer occurs favorably through the dimeric homochiral transitional state, which creates a stereochemical discrimination.

Some Mannich reactions also displayed the enantiomeric enrichment induced by the enantiomerically pure product. The chiral β-aminoketone product of the reaction between acetone and imine (Figure 22) catalyzes its formation.[136] This amine can bind to the imine and can direct the addition of incoming enol. The latter work assumed the alternative transitional state, where imine and the product form an asymmetrically biased 8-membered cycle.[137]

Kawasaki et al. reported asymmetric amplification in amino acid precursor synthesis.[138] Upon mixing HCN p-tolualdehyde and amine, they obtained a mixture of chiral aminonitriles via the Strecker reaction. These aminonitriles can afford enantio-merically enriched solids upon the addition of corresponding chiral aminoacids. Aminonitriles consequently undergo hydrolysis to the corresponding enantipure aminoacids. Later, the same group reported the amplification of a small enantiomeric excess in a similar Strecker reaction by a cyclic temperature regulation that initiates the crystallization-dissolution cycles.[139]
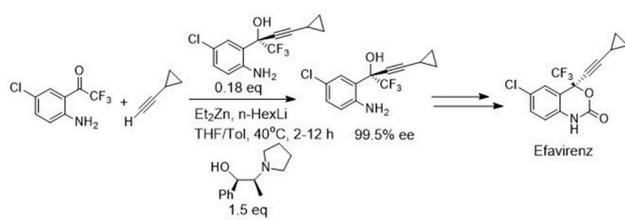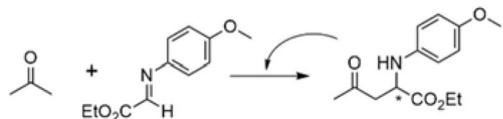
4.5. Other Examples

The photochemical transformation of α-diketone that bridges two aromatic rings into the anthracene derivative is a unique example of photo-autocatalysis (Figure 23).[110a] In this reaction, anthracene, which is a better chromophore than is diketone, photosensitizes its formation. Nitschke and co-workers presented the supramolecular photo-autocatalysis. There, BODIPY-bridged metal-organic cage with imines as a coordination ligand acts as an $^1O_2$ photogeneration agent. Upon imine exchange with iodoaniline it becomes more efficient chromophore. Then initial cage, upon oxidation exchanges with iodoaniline faster, provoking the autocatalytic behavior.[110b] Mirkin and co-workers designed an autocatalysis system using a switchable catalyst.[140] The catalyst is initially in the OFF state, but it switches ON upon reaction with acetate. When in the ON state, it catalyzes the formation of the acetate from starting materials. The acetate formed in this catalytic reaction switches more catalyst from the OFF to the ON state and closes the autocatalytic loop. Perhaps, synthesizing switchable catalysts, as in the previous example, is one of the most general strategies for designing autocatalytic reactions. Interestingly, the Baylis-Hillman reaction – which is a tertiary amine catalyzed addition of conjugated carbonyls to aldehydes – is also weakly autocatalytic because of the stabilization of the transition state of this reaction by its product[112]

In summary, autocatalysis, based on small organic molecules, shows the highest diversity of mechanisms and, consequently, there are many opportunities to develop new autocatalytic systems. This type of reaction is very suitable for designing autocatalytic networks; this represents one of the biggest opportunities in the development of autocatalysis. However, one class of organic reactions plays a special role in

Figure 21. Asymmetric amplification in the synthesis of *Efavirenz*.[133]

Figure 22. The asymmetric autocatalytic Mannich addition.[136,137]
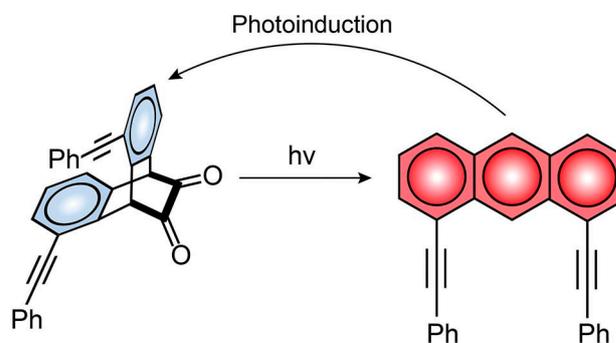
Figure 23. Autocatalytic photoactivated transformation of α-diketone.[110a] Reproduced with permission from Ref. [110a]. Copyright 2016 American Chemical Society.

ChemSystemsChem

Reviews
doi.org/10.1002/syst.202000026

**Chemistry
Europe**
European Chemical
Societies Publishing

autocatalysis – it is template-assisted reactions. In these reactions, the transition state of the autocatalytic path is the subject of design. We will discuss them in the next sections.

5. Autocatalysis Based on the Template Effect

Representative autocatalytic reactions based on the template effect are summarized in Table 3.

5.1. Template-Assisted Autocatalysis via Small-Molecule Chemistry

Information transfer in life-inspired systems is inevitably connected with the concept of a template. The most famous example is the DNA-RNA-protein reaction sequence, where RNA is the template for protein synthesis and DNA is a template for RNA or itself. In biology, enzymes can mediate the efficient transition of information from a template to a product.[141] Nevertheless, replications of nucleotide chains can occur without involving enzymatic catalysis, but the efficiency and quality of this replication are low. With developments in the field of template synthesis, it became possible to direct the assembly of complex organic molecules using molecular templates.

As an example of DNA replication, a template recognizes, attracts, and brings monomers close to each other in a defined order through noncovalent interactions. Information transfer in templated reactions comes from the ordering of the monomers on a template. The catalytic effect of a template comes from

the acceleration of the coupling of monomers near the template.[142,143] If a template is the product of the coupling, the reaction becomes autocatalytic. If the coupling of monomers is reversible, the reaction is thermodynamically controlled.[144,145] If the coupling is irreversible, the reaction is kinetically controlled, which is a necessary condition for Darwinian evolution.

The group of Rebek was the first to develop the concept of template replication for small molecules..[146] Rebek's first self-replicating system (Figure 24) functioned through a templated amidation of perfluorobenzene ester **2**. Recognition units, adenine, and imide (denoted in blue in the scheme) form a hydrogen bond. The reaction proceeds by two pathways: (i) a direct bimolecular reaction between **1** and **2** and (ii) a reaction through the trimolecular complex [**1·2·3**] of products with reactants. Both pathways contribute substantially to product formation. To determine the importance of the templated pathway, Rebek's group disabled it by methylating the imide recognition unit in **3**. The addition of methylated **3** to the reaction did not cause any change in the efficiency of the coupling. However, the addition of inhibitor, 2,6-bis(acylamino) pyridine, which forms a strong hydrogen bond with **2** and **3**, dramatically decreased the rate constant.[147] Menger et al. found another important drawback of Rebek's system.[148] They suggested that amides in the system might be the actual catalysts of the reaction instead of the template. Later, Reinhoudt used the kinetic analysis to dispute this hypothesis. He showed that background processes are negligible compared to the actual bimolecular and tri molecular pathways.

The second generation of replicators (Figure 25) maximizes the contribution of the trimolecular pathway. The efficiency of

Table 3. Representative template-assisted autocatalytic reactions.

Reaction	Autocatalyst	Mechanism	$k_{autocat}$	k_{noncat}	Ref.
Figure 30(a).	Tip of the supramolecular fiber	Fragmentation of the supramolecular stacks			[160]
Figure 27(a)	Coupling product	Templating by hydrogen-bonding	$1.31*10^{-3}$ M^{-2}s^{-1}	$7.43*10^{-5}$ M^{-1}s^{-1}	[157]
Figure 24	Coupling product	Templating by hydrogen-bonding			[146]
	Coupling product	Templating by hydrogen-bonding			[161]
Figure 25	Coupling product	Templating by hydrogen-bonding			[149]
Figure 26(a)	Coupling product	Templating by hydrogen-bonding	0.133 M$^{-1.8}$s^{-1}	$1.3*10^{-4}$ M^{-1}s^{-1}	[151]
Figure 26(b)	Coupling product	Templating by hydrogen-bonding			[154]
Figure 31	Hexanucleotide	Templating by base-pairing	$9.48*10^{-8}$ M$^{1/2}$s^{-1}	$3.87*10^{-9}$ s^{-1}	[26b]
Figure 33	PNA template	Templating by base-pairing	$(1.40 \pm 0.03) \times 10^{-2}$ M$^{-3/2}$s^{-1}	$2.7*10^{-4}$ M$^{-1/2}$	[162]
Figure 34	RNA ligase	Templating by base-pairing			[163]
Figure 36	Oligopeptide	Templating through the coiled coil complex	29.4 ± 0.8 M$^{-3/2}$s^{-1}	0.063 M$^{-1/2}$s^{-1}	[164]
Chmilievski's system	Oligopeptide	Templating through the tetra-meric complex	50.6 M$^{-1.91}$s^{-1}	5.0×10^{-4}	[165]
		Templating through the β-sheet complex			[166]
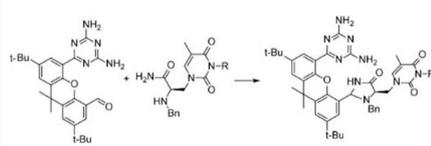
ChemSystemsChem

Reviews
doi.org/10.1002/syst.202000026

Chemistry Europe
European Chemical
Societies Publishing
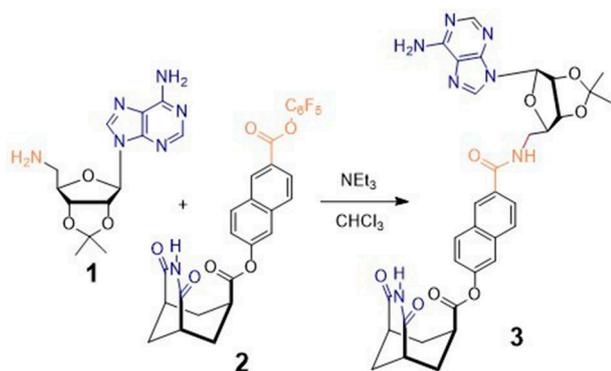
Figure 24. Rebek's first generation self-reproducing system. A reaction occurs between the protected aminoadenosine **1** and perfluorobenzene-activated acid **2** (reactive groups are denoted in orange), forming template **3**. Adenine and imide (in blue) are the recognition units.[146]
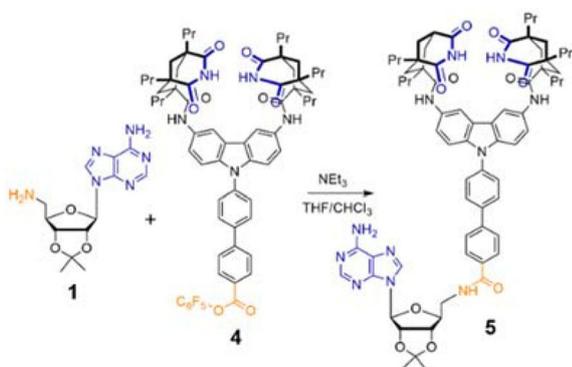
Figure 25. Rebek's second generation of self-reproducing systems. "Molecular clefts" and adenine (in blue) interact via hydrogen bonds. A reaction occurs between the protected aminoadenosine and the perfluorobenzene-activated acid (reactive groups are denoted in orange).[149]

Figure 26. Autocatalytic Diels-Alder reactions by Sutherland and Wang (a)[151] and by von Kiedrowski (b).[154] Green symbolizes the recognition units and orange the reactive groups.

autocatalysis was strongly improved in this system in comparison with the first generation of replicators. Imide "molecular clefts" in compound **4** (blue in the Figure 25), and adenine, in **1**, are the recognition units. The coupling occurs via the same mechanism as in the first generation. Elongation of the spacer between the activated acid and "molecular clefts" in **4** restricts the reaction in the bimolecular complex [**1·4**].[149]

Rebek and co-workers also designed an autocatalytic replicator that serves as the catalyst for other reactions.[150] The replication reaction occurs between the aldehyde containing the melamine recognition block and the thymine-derived 2-aminoacetamide. The product contains an imidazolidinone heterocycle that acts as the catalyst for the Friedel-Crafts reaction and for cinnamaldehyde reduction. The initial rate of this reaction was in the range of μM/min.

Sutherland[151] reported an autocatalytic templated reaction via a kinetically controlled Diels-Alder cycloaddition (Figure 26(a)). He applied two common supramolecular recognition synthons, 2-amidonaphtaridine, in **6**, and 6-amino-2(1H)-pyridinone, in **7** (green in the scheme). This system demonstrated autocatalysis with the order equal to 0.8 and perhaps the

highest autocatalytic efficiency for small-molecular replicators at the time The reaction order on the autocatalyst close to 1 indicates only weak substrate inhibition through the formation of a dimer, probably because of significant structural changes during Diels-Alder cycloaddition. This strategy of avoidance of substrate inhibition will remain the main tool for building efficient self-replicating systems[152,153]

Von Kiedrowski[154] and co-workers reported a reaction that enables control over the diastereoselectivity in Diels-Alder cycloaddition (Figure 26(b)). Hydrogen-bonded interactions control the assembly of building blocks. A cyclopentadiene derivative with a pyridine-amide recognition block (**9**) and a dienophile, maleimide derivative with a carboxylic acid recognition unit (**10**) produced, almost exclusively, one out of four possible diastereomeric products. Cycloaddition results in a 16/1 diastereomeric ratio and a 77% yield of the major product. The molecular simulations for this system showed that the product-product complex dissociation constant is significantly lower than the one for reagent-product complexes. Therefore, significant product inhibition takes place in this reaction.

A system with a reaction similar to an alkyne-azide click-reaction also suffers from the high stability of a template homoduplex. The kinetic study for this reaction did not display a sigmoidal profile.[155] Several Diels-Alder template systems designed by the group of Philp and Kassianidis revealed the difference between endo and exo cycloadducts as templates. An endo product works as a template more efficiently than does an exo product; however, it does so without producing any appreciable autocatalytic kinetics.[156]

Nitrone-alkene [2+3]-cycloaddition (Figure 27, (a)), in comparison to the Diels-Alder coupling pathway, which results in the more selective (exo vs endo) replication with clear sigmoidal kinetics. The selectivity of cycloaddition indicates that the predominantly endo-product (13) acts as a template. By injecting the endo-template and diluting the reaction mixture, the authors achieved a level of exo-product below the detection level. Their computational study concluded that the exo-product has recognition sites in the proximity that does not allow them to interact efficiently with the reagents.[156]

Philp's group[157] demonstrated the propagation of the autocatalytic front in the nitrone-alkene system. A small amount of a template, located at one tip of a syringe, created the front in the solution of its precursors. The effect was visualized by

ChemSystemsChem

Reviews
doi.org/10.1002/syst.202000026

Chemistry
Europe
European Chemical
Societies Publishing
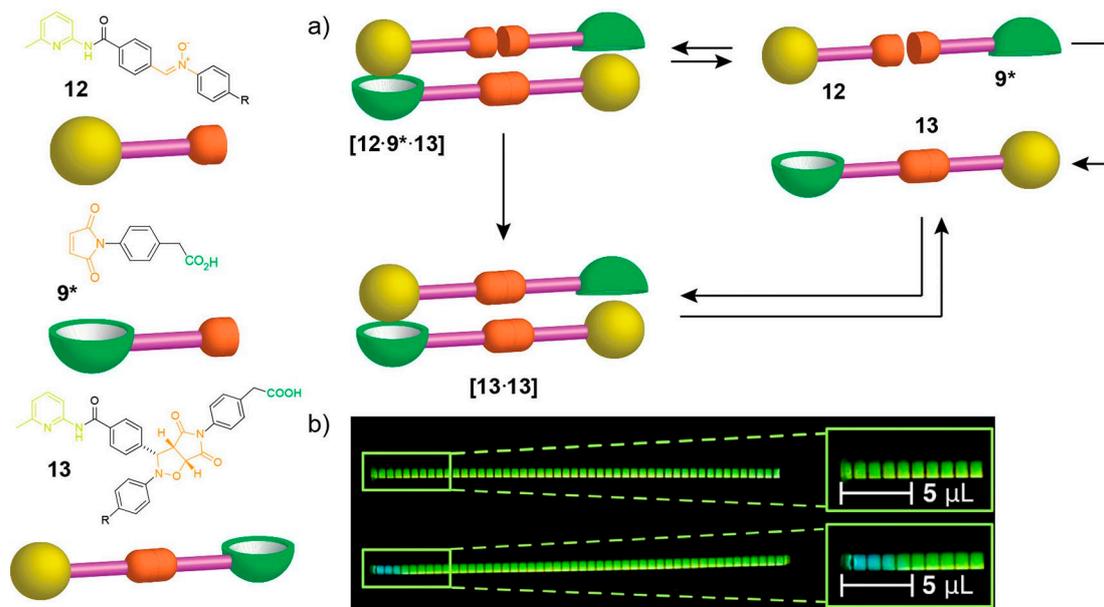
Figure 27. a) Philp's [2+3] autocatalytic cycloaddition system. R=H. Orange denotes the reactive groups (nitrone in 12 and alkene in 9*). The yellow sphere denotes the pyridineamide recognition block and the green cup denotes carboxylic acid. b) The autocatalytic front of the reaction (a) with R=9-ethynylanthracene..,[156,157] Reproduced with permission from Ref. [157]. Copyright 2016 American Chemical Society.

attaching the 9-ethynylanthracene label to the nitrone reagent (Figure 27(b)).

Philp and co-workers designed a system (Figure 28) that generates two replicators (**16** and **17**) that compete with each other for reagent **14**. Carboxylic acid in the meta- and para-positions changes the efficiency of templating by the product. Compound **17** is an excellent template in itself and is moderate for **16**. By contrast, compound **16** is a slower replicator and does not influence the formation of **17**. When **9***, **14**, and **15** were mixed without adding products at the beginning of the experiment, **16** and **17** appeared in nearly equal concentrations. The addition of 20 mol% of template **17** caused its domination
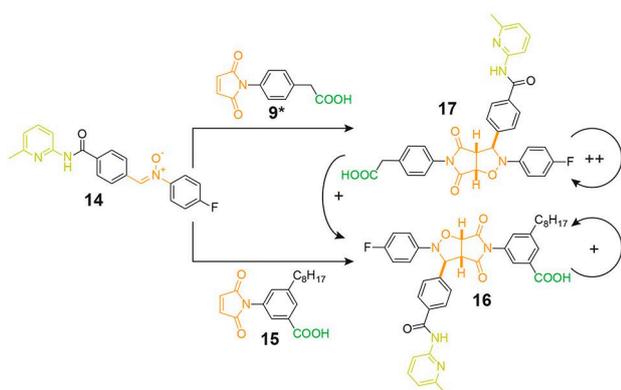
over **16** after a 4 h experiment ([**16**]/[**17**]=0.8). Similarly, the addition of **16** produced its excess ([**16**]/[**17**]=2.38).[158]

Philp and co-workers later created the system, where four aldehydes, one of which contained pyridine-amide, three anilines and hydroxylamine generated the dynamic combinatorial library (DCL), through the condensation reactions. Hydroxylamine reacted with aldehydes, producing the nitrone **14**. Addition of maleimides **9*** and **15** produced templates **16** and **17**. The distribution of the products after 7 days [**16**]/[**17**]=1.2. At the same time, the DCL the amount of all aldehydes diminished, they formed nitrones, in order to replenish the loss of 14 from the equilibrated mixture.[159]

Probably the most complex system in the class emerges from the reagent pool of two nitrones (**18** and **14**) and two maleimides (**9*** and **19**) (Figure 29). Each molecule contains either carboxylic acid or a pyridine-amide group. In the product pool, the compounds have either both recognition groups or two copies of one. Molecules with two different recognition blocks (**21** and **17**) act as replicators. Products **22** and **20** are the cross-catalysts for each other's formation. Interestingly, products **20** and **22** outperformed the other molecules in distributing the product, with and without templates in the reaction mixture. Nevertheless, the number of replicators **17** and **21** increased when any of them was added.[159]

Otto's group developed cyclic disulfide replicators (Figure 30 (a)) that emerged from the dynamic combinatorial library of peptide-substituted 1,3-dithiobenzenes. The system generates oligomeric macrocycles having 3–8 monomers in their composition. However, some macrocycles were autocatalysts and dominated the product pool. Surprisingly, the dominating macrocycles differ, depending on the applied mixing. 6-mer

Figure 28. The system with two competing replicators **16** and **17**. + + denotes a highly active process, + denotes a moderately active process. The catalysis involved in the production of **17** by **16** is negligible. Yellow highlights the pyridineamide groups, green the carboxylic acid, and orange the reactive groups.[158]

ChemSystemsChem

Reviews
doi.org/10.1002/syst.202000026

Chemistry Europe
European Chemical
Societies Publishing

Figure 29. Philp's multicyclic auto- and cross-catalyzed [2 + 3] cycloaddition system. Yellow highlights the pyridineamide groups, green the carboxylic acid, and orange the reactive groups.[159]

emerged as a replicator upon shaking (Figure 30(b)), whereas 7-mer emerged upon stirring.[157]

The microscopy studies showed that macrocycles assemble into the fibers. The termini of these fibers act as templates for the formation of the macrocycles. Shaking or stirring breaks stacks that are longer than some critical length and doubles the number of the termini. Because the rate of growth of stacks is proportional to the concentration of these termini, the growth is autocatalytic: autocatalysts are at the termini of stacks.[167]

Sadownik et al. confirmed that amino acid substitution in the building block can either stabilize or destabilize the fibers.[168] This effect has a substantial influence on the autocatalysis. The researchers used the DCL of 1,3-dithioben-zenes, modified with two peptides, Gly-Leu-Lys-Phe-Lys and Gly-Leu-Lys-Ser-Lys. After oxidation, they observed the preferential formation of macrocycles with phenylalanine, because of its ability to stabilize the fibers by pi-pi interactions. When the serine-rich building blocks were in excess, phenylalanine-rich macrocycles seeded the growth of the serine-rich fibers.

Alanine-based building blocks in 10% TFE (2,2,2-trifluoroe-thanole) in water, assembled the majority of the 8-mers. However, in 17% v/v TFE 6-mer became the major product. Thus, the solvent composition can dramatically change the distribution of the products of this replication. 8-mer and 6-mer seeds in the favored solvent system induced autocatalytic growth. By contrast, 6-mer seed in 10% TFE initiated the growth of 8-mers. 8-mer can also induce 6-mer replication in 30% TFE.[169]

Otto's autocatalytic stacks are perhaps the system that is closest to the existing synthetic chemical systems that fulfil the conditions for Darwinian evolution. The main challenges with this system are the rather limited evolvability and the significant chemical reversibility. Thus, the evolvable parameters are the size and the composition of disulfide rings, which do not provide high information capacity. The reversibility of disulfide
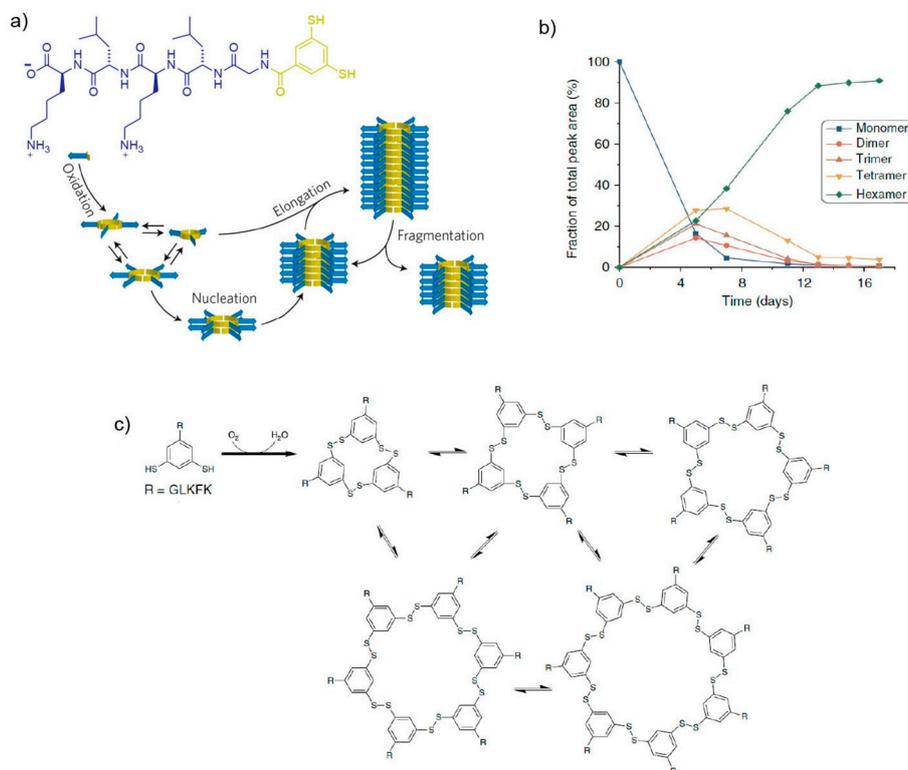
Figure 30. Sijbren Otto's replication system. a) Mechanism of fiber amplification; the arrows denote the polypeptides. b) Macrocycles' distribution over time, displaying amplification of 6-mers. c) The reaction scheme of dithiol oxidation, leading to the oligomeric macrocycles.[167] Copyright permission obtained for relevant sections in this figure? Reproduced/adapted with permission from Ref. [5c]. Copyright 2015 Springer Nature.

ChemSystemsChem

Reviews
doi.org/10.1002/syst.202000026

**Chemistry
Europe**
European Chemical
Societies Publishing

linkers may hamper the system's ability to retain information gained during the evolutionary process.

Nevertheless, small-molecular replicators by definition have very limited information capacity because of their small size. In the next section, we will look into polymeric replicators that potentially have infinite information capacity.

5.2. Template-Assisted Autocatalysis via Nucleic Acids and Peptides

The nucleic acids and peptides are the natural templates to construct autocatalytic systems. The non-enzymatic nucleic acid and peptide replications have been the target of intense research for the past 40 years. The number of works on this subject is large and here we only describe examples representing different mechanisms of autocatalysis. For the more comprehensive overview on this subject we refer reader to the reviews by Orgel,[12a] Holliger,[170] Chmielewski,[165] and Lynn[171]

Von Kiedrowski et al. were one of the first to demonstrate the ability of a simple system containing short template strands to perform self-replication without the presence of enzymes.[26b] His original system was based on G−C pairing, accommodating two complementary trinucleotides C−C−G and G−C−C, a self-complementary template product of their condensation, and an activator of condensation. The system showed an ability to use the product as a catalyst for its formation (Figure 31). The order of this reaction is 0.5. It shows the parabolic growth because of inhibition through the formation of dimers. In another pioneering study,[26c] Kiedrowski's group designed the autocatalytic system based on complementary (but not self-complementary) hexanucleotide templates. This system was perhaps the first rationally designed autocatalytic network since neither of the complementary hexanucleotides is autocatalytic on its own, but only their combination forms an autocatalytic network. The growth of hexanucleotides followed parabolic law, which prevented Darwinian evolution in this system.

Another pioneering research was led by Zielinski et al.[18] They showed results similar to those of Kiedrowski using dimers as substrates. In their experiments, nucleic acid-like oligomers formed complementary tetramers in the presence of an initial amount of the tetramer (Figure 32). The addition of the tetramer template increased the rate of production of new tetramer molecules. A square-root growth of the total concentration of the tetramer comes from the stability of the complementary mini duplex with the tetramer.

Short peptide nucleic acid strands (Figure 33) are also capable of autocatalytic self-replication.[162]

The design of this system is similar to the earlier examples of self-replicating nucleic acids, with the exception of using two PNA molecules in the condensation reaction. The ligation undergoes the activation of the first building block. Template
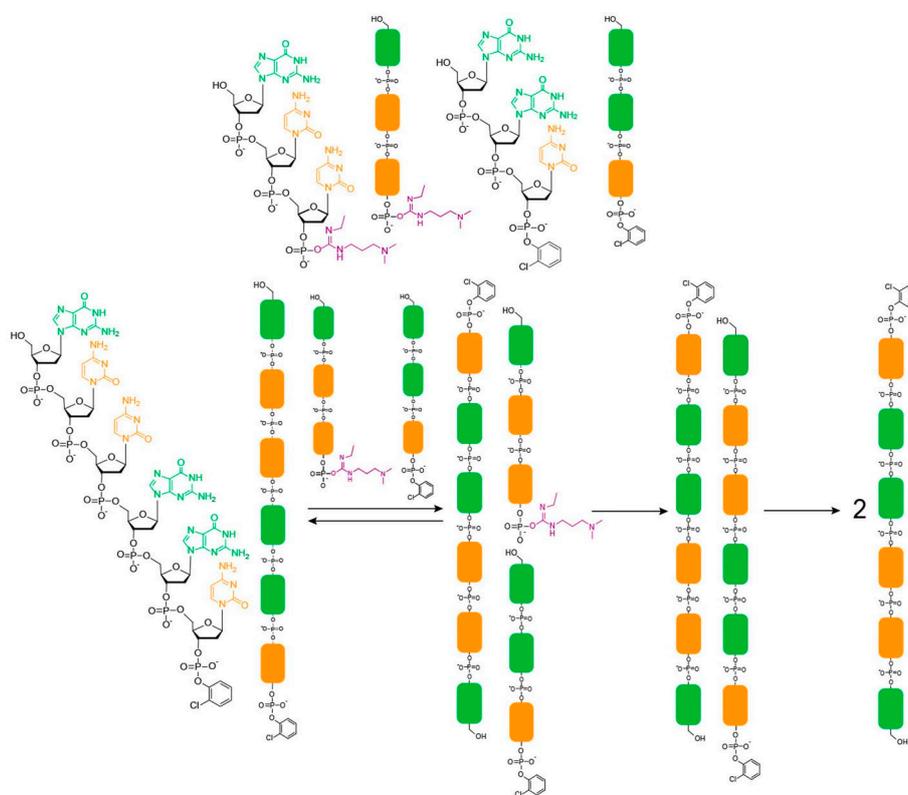
Figure 31. Two complementary trinucleotides condense in the presence of a small amount of the template oligonucleotide. They form a two-stranded complex, allowing starting trinucleotides to react, thus creating a self-complementary duplex.[26b] Reproduced with permission from Ref. [26b]. Copyright 1986 Wiley-VCH.

ChemSystemsChem

Reviews
doi.org/10.1002/syst.202000026

Chemistry
Europe
European Chemical
Societies Publishing
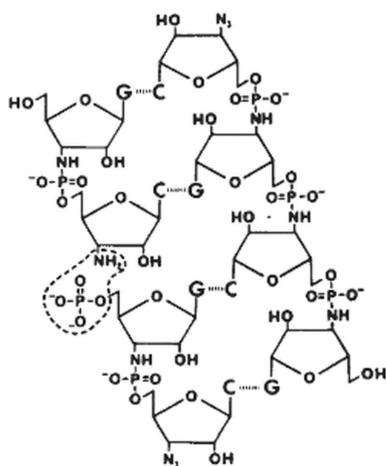
Figure 32. The tetramer in which template condensation occurs.[18] Reproduced with permission from Ref. [18]. Copyright 1987 Springer Nature.

strand conFigure blocks form a complex, allowing them to perform condensation, resulting in two template strands in the system, releasing one from the system and repeating the process.

Although it is not a purely synthetic system, the self-replicating RNA reported by Lincoln and Joyce is a classic example of evolution driven by autocatalysis. They studied systems based on R3C RNA ligase,[173] which binds two oligonucleotides through Watson-Crick pairing and catalyzes the reaction between them, forming a 3',5'-phosphodiester. In this study, oligonucleotides are halves of the R3C ligase and its negative R3C' (according to Watson-Crick pairing). Therefore, R3C replicates R3C' and R3C' replicates R3C, making the overall system autocatalytic (Figure 34).

The production rates of the resulting **EE'** complexes were tenfold lower than those of the initial R3C ligase. The low efficiency was explained by the slow dissociation of the complex. Then the catalytic properties of the enzyme were improved by in vitro evolution, letting nucleotides randomize in the sequence. Populations of enzymes were allowed to perform six rounds of selection based on the rate of replication, after which the resulting enzymes were cloned. With new, more catalytically active enzymes, it was possible to achieve the reaction with exponential growth. For an example of a complex network of RNA ligations, we refer the reader to a seminal work by Lehman et al.[174]

Figure 34. The modified enzyme E' binds A and B oligonucleotides through Watson-Crick interaction and catalyzes the reaction between them, forming a copy of enzyme E, resulting in complex EE'. The complex EE' dissociates, releasing a new enzyme molecule E in a free state, whereas E catalyzes the ligation between A' and B', forming E', creating an autocatalytic cycle. Reproduced from Ref. [173] with permission. Copyright 2009 American Association for the Advancement of Science.

Szostak and co-workers work on the enzyme-free self-replication of RNA molecules in vesicles.[175] They created an efficient system for enzyme-free RNA replication by activating phosphate with methylimidazole and utilizing 5'-activated oligonucleotides as catalysts (Figure 35).[176]

Lee et al. showed an example of the self-replication of peptides.[164] In contrast to nucleic bases, amino acids do not form complementary hydrogen bonds. Templating by peptides requires a well-defined secondary structure (e.g., an α-helix or a β-sheet) for the template. In addition, the core of the experiment stays the same as for oligonucleotides. Ghadiri used oligopeptides that form α-helixes, which coil around each other. This coiling is the basis for the template's effect in this system (Figure 36).

Figure 33. Peptide nucleic acid strands used in the experiment.[162] Reproduced from Ref. [162] with permission. Copyright 2014 Royal Society of Chemistry.
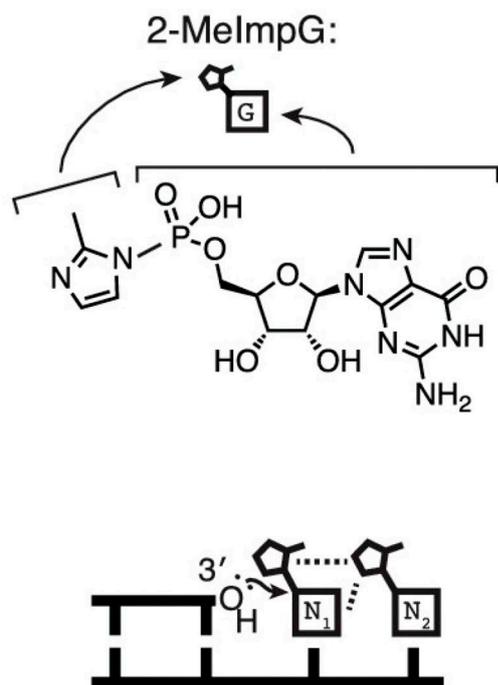
Figure 35. Szostak's non-enzymatic primer extension mechanism. On the top is the structure of 2-methylimidazole that activates guanosine monophosphate. On the bottom is a schematic representation of a primer with 3'-OH that attacks the activated nucleotide. **N1** is the complementary nucleotide, **N2** is the downstream nucleotide, facilitating the coupling.[176a] Reproduced from Ref. [176a] with permission. Coyright 2016 The Authors.
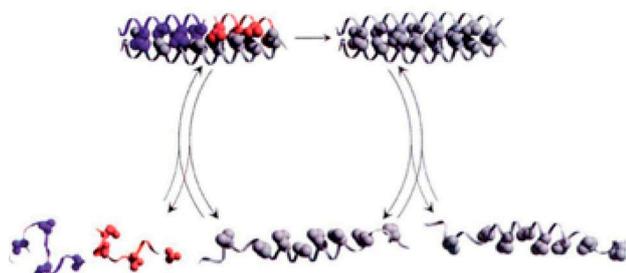
Figure 36. Schematic process of an autocatalytic cycle showing the formation of new alpha helixes from the electrophile (blue, COSBn residue), nucleophile (red, amine residue), and a template protein chain (gray). The templating process is based on specific inter-helical hydrophobic interaction.[164] Reproduced from Ref. [164] with permission. Copyright 1996 Springer Nature.

The system was built from structures that consisted of 32 amino acid chains, which can be schematically described as a repeating (abcdefg)n pattern. Those peptides form coiled coils via hydrophobic interactions between the surfaces formed by alkyl residues of leucine and valine. One of oligopeptides was terminated with the thioester group and another one with cysteine, allowing them to couple through the native chemical ligation. The self-replication process displays a parabolic growth pattern, with the initial rates of product formation being proportional to the square root of the template concentration.

The Ghadiri's replicators lack the autocatalytic sigmoidal profile because of two reasons: high stability of the coiled coil structure of the product and strong contribution of the background ligation reactions. Chmielewski and co-workers achieved sigmoidal kinetic profiles with the same ligation chemistry. Their design aimed to disrupt the formation of coiled-coils by using a shorter 26 amino acid peptide with the pH-sensitive glutamate regions next to the hydrophobic surface. The last factor decreased the degree of helicity of a peptide. Overall, they accomplished efficient replication in tetrameric complexes with the low contribution of background mechanisms.[177]

Ghadiri's group also used the same principle of helical templating to design an autocatalytic network of oligopeptide replicators (Figure 37).[178] Three starting peptides, one thioester-terminated and two cysteine-terminated, form two ligation products that can act as templates. They, however, do not act as templates for their own production – only for another template. This results in a cross-catalytic network that corresponds to the network structure from Figure 3b (with only two catalysts, A and B).

Ashkenasy et al. described the formation of chemical reaction networks based on a templated replication of oligopeptides.[170] As in the previous example, the ligation reaction occurred between two peptide fragments: one terminated with thioester and one terminated with cysteine, which formed a coil-coiled structure with a template. The experimental network consisted of eight nodes from nine templates.[179a] These nodes were connected by 14 directed edges. The experimental network was, however, substantially smaller than the theoretically predicted network that consisted of 25 nodes and 53 directed edges (Figure 38). Interestingly, this model network somewhat resembled the scale-free networks that characterize the protein-protein interactions in biological systems.

Not only were long-chained coil-coiled helical protein templates studied.
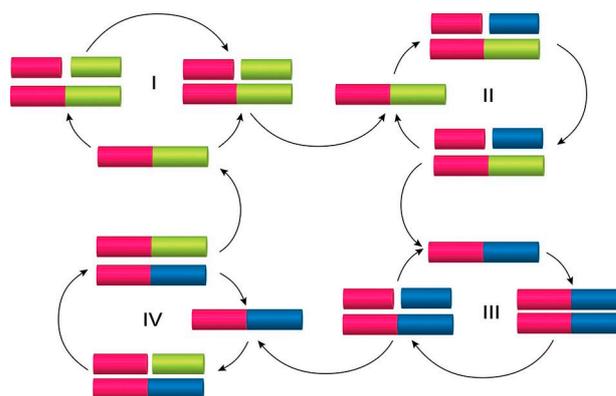
Figure 37. Ghadiri's autocatalytic network. The network consists of four catalytic cycles, two templates, and three starting peptides. Red rectangles denote thioester-terminated peptides; blue and yellow denote cysteine-terminated peptides. Mixed colored rectangles are the products of their coupling.[178] Reproduced with permission from Ref. [178]. Copyright 1997 Springer Nature.

ChemSystemsChem

Reviews
doi.org/10.1002/syst.202000026

**Chemistry
Europe**
European Chemical
Societies Publishing

Figure 38. Calculated graph illustrating the formation of a self-organized peptide network composed of 25 nodes joined by 53 vector edges. Each node represents a product template sequence. The directed edges signify the ligation pathways and the curved arrows indicate autocatalysis[179a] Reproduced with permission from Ref. [179a]. Copyright (2004) National Academy of Sciences, U.S.A.

Ashkenasy's group utilized a high tendency of β-sheets to form large molecular assemblies. Rubinow et al. showed that β-sheet aggregates could display enzyme-free self-replication (Figure 39).[166] A beta-sheet water-soluble structure was achieved by combining repetitive dyads of hydrophobic phenylalanine and hydrophilic glutamate residues (Figure 40). The terminal proline acts as a beta-sheet breaker because it does

Figure 39. An autocatalytic cycle resulting in the synthesis of the template peptide. Template production undergoes the ligation reaction between thioester terminated oligopeptide **E** and the cysteine terminated oligopeptide **N**.[179b] Reproduced from Ref. [179b] with permission. Copyright 2008 Wiley VCH.

Figure 40. Template peptide formed by the condensation of E and N through the chemical ligation.[179b] Reproduced from Ref. [179b] with permission. Copyright 2008 Wiley VCH.

Figure 41. The prion conformer operates as a template for the formation of itself from a normally folded protein, and these prions become new templates for a further autocatalytic cycle.[181] Reproduced from Ref. [181] with permission. Copyright 2005 Springer Nature.

not have an N–H group for hydrogen bonding. Therefore, prolines in the sequence were replaced by the capping 4-acetamidobenzoate (ABA). Replication occurred with a clear sigmoidal kinetic profile. Later mechanistic studies suggested that the reaction occurs primarily through transient fibrilic molecular aggregates.[180] We notice that because of the lack of universal complementary pairing, general information coping and evolvability are harder to achieve in oligopeptide- than in oligonucleotide-based systems.

Prions work as a template, creating a chain reaction that spreads the disease (Figure 41).[181] The self-replication process of prions differs from the mechanism underlying the formation of other peptides. Prions are abnormal proteins known to generate several lethal diseases such as Creutzfeldt-Jakob disease (CJD) or Gerstmann-Sträussler-Scheinker syndrome. Prions have an unusual tertiary structure that can convert an identical amino acid sequence of usual proteins into the prion's conformational form, performing a self-replicative behavior. The process of structure conversion is dictated by kinetic and thermodynamic barriers and is unlikely for most proteins. When changed, "the seed" takes another normal conformer, increases in size, forms an amyloid fiber, and repeats the cycle. The fragmentation of fibers stimulates the spreading of the infection.

In conclusion, despite the significant progress in the development of synthetic polymeric replicators, the problem of synthesizing of exponential, information-carrying, polymeric replicator remains open.

6. Designing New Autocatalytic Reactions

The first autocatalytic reactions resulted from serendipitous findings. Nevertheless, autocatalytic reactions can be rationally designed. Various examples of rationally designed autocatalytic systems were discussed in previous sections. Autocatalytic reaction networks and template-assisted reactions are the most suitable ones for the design. In the case of template-assisted reactions, the design target is secondary interactions between substrates, templates, and products. The template-assisted self-replication is a well-developed area; thus, we refer the reader to excellent reviews by Rebek and Philp for detailed discussions of the implementation of template-assisted self-replication.[143,12,182] Less attention was devoted to design strategies for autocatalytic reaction networks than for template-assisted synthesis. In this review, we would like to discuss three strategies that we and others found in practice helpful in designing autocatalytic reaction networks. Generally, one starts this design by drawing a network structure (see Figs. 3 and 4 for examples). However, the number of possible networks is infinite; finding specific reactions that would form the desired network is often extremely difficult.

The first approach is to search for a branched structure for the network (Figure 42a). Many autocatalytic reaction networks can be described as branched-chain reactions. The thioester autocatalytic network,[22] Meldrum's acid-based autocatalytic network,[89] the formose reaction,[8c,120] the formaldehyde-sulfite

Figure 42. Chemical reaction network motifs useful for designing autocatalytic reactions. A) Branched network. B) Ligand-enhanced metal catalysis. C) Destruction of the inhibitor. Red letters denote autocatalysts, blue letters denote important intermediates, and black letters denote starting materials or final products. Black solid arrows denote non-catalytic reactions, black dashed arrows denote catalysis, and gray dashed arrows denote sequences of any reactions.

reaction,[24] and the autocatalytic CuAAC with Cu(II) salts all can be described by this structure.[23] The design of the thioester autocatalytic network is a good example of applying the branching structure. Although this network can be represented by the motif in Figure 3c,[25] finding a catalytic cycle in this system is nontrivial. By contrast, the branching in this reaction is straightforward – the reaction of the thioester with cysteamine generates two thiol molecules from one (Figure 14). It is possible to see this reaction as a nucleophilic chain reaction where the concentration of the strongest nucleophile in the system (thiolate) grows exponentially. Importantly, at least one step in the branched network has to be irreversible.

The second approach is the catalytic formation of a ligand that enhances the catalytic activity of a metal catalyzing the formation of this ligand (Figure 42b). The simple (without the Cu(II) to Cu(I) reduction) of autocatalytic CuAAC is a good example of this class.[97,98a] The triazolyl ligand enhances the catalytic activity of Cu(I), which is a catalyst for its synthesis.

The third approach is the catalytic destruction of an inhibitor for the catalyst (Figure 42c). The group of Huck has recently introduced this strategy for constructing positive feedback in the systems based on proteases.[183] They designed oligopeptide inhibitors for trypsin, chymotrypsin, and elastase. Each oligopeptide contained an amide bond that can be recognized and cleaved by the corresponding protease. Initially, no reaction occurred in the mixture of a protease and its inhibitor because the protease was fully inhibited. Nevertheless, when a protease started to cleave an inhibitor, more protease became active and it cleaved the inhibitor faster, creating a positive feedback loop.

7. Summary and Outlook

The complexity of biological entities, which are self-replicating and autocatalytic, illustrates the gap between what is possible and what was done in the lab for autocatalytic and self-replicating systems. We will discuss three major directions where research on autocatalysis can expand and be enhanced.

The search for prebiotic autocatalytic reaction networks is the first challenging area. Historically, autocatalysis was a core element of research on the origin of life because it is at the core of two problems in most hypotheses on the origin of life:

dilution and prebiotic evolution. Most of the plausible scenarios for the emergence of life require reasonably high concentrations of specific compounds (e.g., activated nucleotides for the RNA world scenario).[184] However, random reactions on prebiotic Earth are more likely to result in a complex mixture of many compounds, each of which is in a low concentration. The autocatalytic reactions can selectively accelerate the production of compounds that are part of an autocatalytic cycle and deplete other pathways from starting materials. Thus, molecules that are part of an autocatalytic system will be presented in high concentrations. The formose reaction is the only autocatalytic reaction with clear prebiotic relevance as a source of sugars.[8c,185] Thus, finding new prebiotic autocatalytic networks will enhance our understanding of chemistry in the prebiotic world. The main challenge lies in a large number of theoretically possible autocatalytic networks, combined with the lack of kinetic information on prebiotic reactions. One of the approaches to this problem might be to collect quantitative information on the kinetics of the elemental reactions of prebiotic relevance in a single database and to use computer algorithms (e.g., as in chematica)[186] to search for autocatalytic networks among these reactions.

Designing a chemical system capable of open-ended Darwinian evolution is the second big challenge. Although we just mentioned evolution, this challenge goes beyond prebiotic chemistry. In our opinion, the right approach is not to restrict this research only to prebiotic chemistry because the task is already extremely difficult without any restrictions. Nevertheless, as soon as we have an example of an evolvable system, we will be able to imagine how similar systems could be constructed based on prebiotic chemistry. To be capable of open-ended evolution, a system should have potentially an infinite diversity of kinetically stable products (such as nucleic acids and proteins in biology), high efficiency, and selectivity of autocatalysis (such as transcription and translation in biology).[32a] Unfortunately, none of the existing synthetic systems can completely fulfill these conditions. The key to resolving this problem might be to combine specific recognition as in template replication with the high catalytic efficiency of nucleophilic or metal catalysis.

The third challenge is applying autocatalysis in materials science. We could utilize autocatalysis to create materials with intricate structures or engineer unique responsive properties into materials.[187] Pojman studied frontal polymerization driven by a heat front or from various autocatalytic reactions.[188] The next interesting step might be to destabilize this front for the synthesis of complex intricate structures such as fractal trees. Autocatalysis is an element of bistable and oscillatory chemical systems,[22,189] as well as systems that form Turing patterns.[190] Thus, Tan et al. proposed the Turing mechanism for the formation of a porous polymer membrane with an entangled structure.[191] Naturally, autocatalytic reactions can be amplifiers of chemical signals and, as part of bistable reaction networks, chemical switches in smart responsive materials.[192] Further development of smart materials will require autocatalytic reactions tailored to specific needs and that are compatible with different chemistries.

Clearly, many more opportunities for research in autocatalytic systems exist than we covered in this article. We hope that with the development of systems chemistry, many exciting discoveries will emerge in the field of autocatalysis.

Conflict of Interest

The authors declare no conflict of interest.

[1] R. Plasson, A. Brandenburg, L. Jullien, H. Bersini, *J. Phys. Chem. A* **2011**, *115*, 8073–8085.

[2] H. Ito, *IBM J. Res. Dev.* **1997**, *41*, 69–80.

[3] G. O. Mallory, J. B. Hajdu, American Electroplaters and Surface Finishers Society, *Electroless plating : fundamentals and applications*, The Society, Orlando, FL, **1990**.

[4] T. H. James, C. E. K. Mees, *The Theory of the photographic process*, 4th ed., Macmillan, New York, **1977**.

[5] a) R. F. Ludlow, S. Otto, *Chem. Soc. Rev.* **2008**, *37*, 101–108; b) G. Ashkenasy, T. M. Hermans, S. Otto, A. F. Taylor, *Chem. Soc. Rev.* **2017**, *46*, 2543–2554; c) E. Mattia, S. Otto, *Nat. Nanotechnol.* **2015**, *10*, 111–119.

[6] a) C. De Duve, *Singularities Landmarks on the Pathways of Life*, Cambridge University Press, Cambridge, UK, **2005**; b) C. De Duve, *Blueprint for a cell : the nature and origin of life*, N. Patterson, Burlington, N. C., **1991**; c) A. Pross, R. Pascal, D. Sutherland, *Open* **2013**, *3*, 120190; d) J. W. Szostak, *Nature* **2009**, *459*, 171–172; e) F. J. Dyson, *Origins of life*, Cambridge University Press, Cambridge Cambridgeshire ; New York, **1985**.

[7] a) A. Pross, *Origins Life Evol. Biospheres* **2004**, *34*, 307–321; b) G. F. Joyce, J. W. Szostak, *Cold Spring Harbor Perspect. Biol.* **2018**, *10*; c) L. E. Orgel, *Acc. Chem. Res.* **1995**, *28*, 109–118.

[8] a) H. J. Morowitz, J. D. Kostelnik, J. Yang, G. D. Cody, *Proc. Natl. Acad. Sci. USA* **2000**, *97*, 7704–7708; b) D. Y. Zubarev, D. Rappoport, A. Aspuru-Guzik, *Sci. Rep.* **2015**, 5:8009; c) A. M. Boutlerow, *C. R. Chim.* **1869**, *53*, 145–147.

[9] a) A. M. Zhabotinsky, *Biofizika* **1964**, *9*, 306–311; b) B. P. Belousov, *Sbornik Referatov po Radiatsionni Meditsine* **1958**, *145*.

[10] V. Castets, E. Dulos, J. Boissonade, P. Dekepper, *Phys. Rev. Lett.* **1990**, *64*, 2953–2956.

[11] a) I. R. Epstein, J. A. Pojman, *An introduction to nonlinear chemical dynamics : oscillations, waves, patterns, and chaos*, Oxford University Press, New York, **1998**; b) I. R. Epstein, B. Xu, *Nat. Nanotechnol.* **2016**, *11*, 312–319.

[12] a) L. E. Orgel, *Nature* **1992**, *358*, 203–209; b) B. G. Bag, G. von Kiedrowski, *Pure Appl. Chem.* **1996**, *68*, 2145–2152; c) T. Kosikova, D. Philp, *Chem. Soc. Rev.* **2017**, *46*, 7274–7305; d) J. Huck, D. Philp, in *Supramolecular Chemistry*, **2012**; e) A. Robertson, A. J. Sinclair, D. Philp, *Chem. Soc. Rev.* **2000**, *29*, 141–152; f) G. Clixby, L. Twyman, *Org. Biomol. Chem.* **2016**, *14*, 4170–4184; g) N. Paul, G. F. Joyce, *Curr. Opin. Chem. Biol.* **2004**, *8*, 634–639; h) K. Soai, T. Kawasaki, A. Matsumoto, *Symmetry* **2019**, *11*, 694; i) D. G. Blackmond, *Chem. Rev.* **2019**; j) D. G. Blackmond, *Cold Spring Harbor Perspect. Biol.* **2019**, *11*; k) S. B. Tsogoeva, *J. Syst. Chem.* **2010**, *1*, 8; l) K. Soai, T. Kawasaki, A. Matsumoto, *Acc. Chem. Res.* **2014**, *47*, 3643–3654; m) T. Kawasaki, K. Soai, *Isr. J. Chem.* **2012**, *52*, 582–590; n) K. Soai, T. Shibata, I. Sato, *Acc. Chem. Res.* **2000**, *33*, 382–390.

[13] A. J. Bissette, S. P. Fletcher, *Angew. Chem. Int. Ed.* **2013**, *52*, 12800–12826; *Angew. Chem.* **2013**, *125*, 13034–13061.

[14] G. A. M. King, *Chem. Soc. Rev.* **1978**, *7*, 297–316.

[15] a) N. Wagner, G. Ashkenasy, *J. Chem. Phys.* **2009**, *130*, 164907; b) N. Wagner, G. Ashkenasy, *Isr. J. Chem.* **2015**, *55*, 880–890.

[16] P. Gray, S. K. Scott, *Chem. Eng. Sci.* **1983**, *38*, 29–43.

[17] P. Schuster, *Monatsh. Chem.* **2019**, *150*, 763–775.

[18] W. S. Zielinski, L. E. Orgel, *Nature* **1987**, *327*, 346–347.

[19] a) H. F. Launer, *J. Am. Chem. Soc.* **1932**, *54*, 2597–2610; b) H. F. Launer, D. M. Yost, *J. Am. Chem. Soc.* **1934**, *56*, 2571–2577.

[20] R. Breslow, *Tetrahedron Lett.* **1959**, 22–26.

[21] C. N. Hinshelwood, *J. Chem. Soc.* **1952**, 745–755.

[22] S. N. Semenov, L. J. Kraft, A. Ainla, M. Zhao, M. Baghbanzadeh, C. E. Campbell, K. Kang, J. M. Fox, G. M. Whitesides, *Nature* **2016**, *537*, 656–660.

[23] S. N. Semenov, L. Belding, B. J. Cafferty, M. P. Mousavi, A. M. Finogenova, R. S. Cruz, E. V. Skorb, G. M. Whitesides, *J. Am. Chem. Soc.* **2018**, *140*, 10221–10232.

[24] M. G. Burnett, *J. Chem. Educ.* **1982**, *59*, 160.

[25] E. V. Skorb, S. N. Semenov, *Life (Basel)* **2019**, *9*, 42.

[26] a) E. Szathmary, *Philos. Trans. R. Soc. London Ser. B* **2006**, *361*, 1761–1776; b) G. Von Kiedrowski, *Angew. Chem. Int. Ed. Engl.* **1986**, *25*, 932–935; c) D. Sievers, G. von Kiedrowski, *Nature* **1994**, *369*, 221–224; d) G. von Kiedrowski, *Bioorg. Chem. Front.*, **1993**, 3, 113–146.

[27] S. Lifson, H. Lifson, *J. Theor. Biol.* **1999**, *199*, 425–433.

[28] R. Aris, P. Gray, S. K. Scott, *Chem. Eng. Sci.* **1988**, *43*, 207–211.

[29] a) S. A. Kauffman, *J. Theor. Biol.* **1986**, *119*, 1–24; b) S. A. Kauffman, *The origins of order : self-organization and selection in evolution*, Oxford University Press, New York, **1993**.

[30] D. G. Blackmond, *Angew. Chem. Int. Ed.* **2009**, *48*, 386–390; *Angew. Chem.* **2009**, *121*, 392–396.

[31] a) R. Plasson, H. Bersini, *J. Phys. Chem. B* **2009**, *113*, 3477–3490; b) S. Schuster, C. Hilgetag, *J. Phys. Chem.* **1995**, *99*, 8017–8023.

[32] a) M. Eigen, *Naturwissenschaften* **1971**, *58*, 465–523; b) M. Eigen, P. Schuster, *Naturwissenschaften* **1977**, *64*, 541–565; c) M. Eigen, P. Schuster, *Naturwissenschaften* **1978**, *65*, 7–41; d) M. Eigen, P. Schuster, *Naturwissenschaften* **1978**, *65*, 341–369.

[33] a) E. Szathmáry, I. Gladkih, *J. Theor. Biol.* **1989**, *138*, 55–58; b) E. Szathmáry, *Trends Ecol. Evol.* **1991**, *6*, 366–370; c) V. Vasas, C. Fernando, M. Santos, S. Kauffman, E. Szathmary, *Biol. Direct* **2012**, *7*, 1.

[34] a) P. Schuster, K. Sigmund, R. Wolff, *J. Math. Chem.* **1980**, *78*, 88–112; b) P. F. Stadler, P. Schuster, *Bull. Math. Biol.* **1990**, *52*, 485–508; c) B. M. Stadler, P. F. Stadler, P. Schuster, *Bull. Math. Biol.* **2000**, *62*, 1061–1086.

[35] S. Lifson, *J. Mol. Evol.* **1997**, *44*, 1–8.

[36] F. J. Dyson, *J. Mol. Evol.* **1982**, *18*, 344–350.

[37] a) D. Segré, D. Lancet*, O. Kedem, Y. Pilpel, *Origins Life Evol. Biospheres* **1998**, *28*, 501–514; b) D. Segre, D. Ben-Eli, D. Lancet, *Proc. Natl. Acad. Sci. USA* **2000**, *97*, 4112–4117; c) O. Markovitch, D. Lancet, *Artif. Life* **2012**, *18*, 243–266; d) D. Lancet, R. Zidovetzki, O. Markovitch, *J. R. Soc. Interface* **2018**, *15*, 20180159.

[38] a) W. Hordijk, J. Hein, M. Steel, *Entropy* **2010**, *12*, 1733–1742; b) W. Hordijk, M. Steel, S. Kauffman, *Acta Biotheor.* **2012**, *60*, 379–392; c) P. Nghe, W. Hordijk, S. A. Kauffman, S. I. Walker, F. J. Schmidt, H. Kemble, J. A. M. Yeates, N. Lehman, *Mol. BioSyst.* **2015**, *11*, 3206–3217; d) W. Hordijk, M. Steel, *BioSystems* **2017**, *152*, 1–10; e) W. Hordijk, M. Steel, P. Dittrich, *New J. Phys.* **2018**, *20*, 015011; f) W. Hordijk, S. Shichor, G. Ashkenasy, *ChemPhysChem* **2018**, *19*, 2437–2444; g) M. Steel, W. Hordijk, J. C. Xavier, *J. R. Soc. Interface*, **2019**, *16*, 20180808.

[39] G. von Kiedrowski, E. Szathmáry, *Selection* **2001**, *1*, 173–180.

[40] a) J. D. Farmer, S. A. Kauffman, N. H. Packard, *Physica* **1986**, *22*, 50–67; b) W. Hordijk, *Biol. Theory* **2019**, *14*, 224–246.

[41] K. A. Kovács, P. Gróf, L. Burai, M. Riedel, *J. Phys. Chem. A* **2004**, *108*, 11026–11031.

[42] J. F. Perez-Benito, C. Arias, E. Brillas, *Int. J. Chem. Kinet.* **1990**, *22*, 261–287.

[43] J. F. Perez-Benito, *J. Phys. Chem. C* **2009**, *113*, 15982–15991.

[44] a) J. F. Perez-Benito, F. Mata-Perez, E. Brillas, *Can. J. Chem.* **1987**, *65*, 2329–2337; b) J. de Andres, E. Brillas, J. A. Garrido, J. F. Perez-Benito, *J. Chem. Soc. Perkin Trans. 2* **1988**, *2*, 107–112.

[45] S. A. Farokhi, S. T. Nandibewoor, *Can. J. Chem.* **2004**, *82*, 1372–1380.

[46] R. J. Field, E. Koros, R. M. Noyes, *J. Am. Chem. Soc.* **1972**, *94*, 8649–8664.

[47] L. Gyorgyi, T. Turanyi, R. J. Field, *J. Phys. Chem.* **1990**, *94*, 7162–7170.

[48] M. Endo, S. Abe, Y. Deguchi, T. Yotsuyanagi, *Talanta* **1998**, *47*, 349–353.

[49] F. Rossi, M. A. Budroni, N. Marchettini, L. Cutietta, M. Rustici, M. L. T. Liveri, *Chem. Phys. Lett.* **2009**, *480*, 322–326.

[50] L. P. Tikhonova, *React. Kinet. Catal. Lett.* **1990**, *42*, 367–373.

[51] I. R. Epstein, K. Kustin, L. J. Warshaw, *J. Am. Chem. Soc.* **1980**, *102*, 3751–3758.

[52] I. Lengyel, T. Barna, G. Bazsa, *J. Chem. Soc.* **1988**, *84*, 229–236.

[53] I. Lengyel, I. Nagy, G. Bazsa, *J. Phys. Chem.* **1989**, *93*, 2801–2807.

[54] E. Abel, H. Schmid, J. Weiss, *Z. Phys. Chem.* **1930**, *147*, 69–86.

[55] M. N. Hughes, E. D. Phillips, G. Stedman, P. A. E. Whincup, *J. Chem. Soc. A* **1969**, *0*, 1148–1151.

[56] J. R. Pembridge, G. Stedman, *J. Chem. Soc. Dalton Trans.* **1979**, *11*, 1657–1663.

[57] G. Bazsa, I. R. Epstein, *Comments Inorg. Chem.* **1986**, *5*, 57–87.

[58] R. H. Simoyi, *J. Phys. Chem.* **1985**, *89*, 3570–3574.

[59] G. Rabai, M. T. Beck, *Inorg. Chem.* **1987**, *26*, 1195–1199.

[60] J. N. Figlar, D. M. Stanbury, *J. Phys. Chem. A* **1999**, *103*, 5732–5741.

[61] R. H. Simoyi, I. R. Epstein, *J. Phys. Chem.* **1987**, *91*, 5124–5128.

[62] V. Francisco, L. Garcia-Rio, J. António Moreira, G. Stedman, *New J. Chem.* **2008**, *32*, 2292–2298.

[63] S. P. Tanner, *Inorg. Chem.* **1978**, *17*, 600–606.

[64] C. J. Gerdts, D. E. Sharoyan, R. F. Ismagilov, *J. Am. Chem. Soc.* **2004**, *126*, 6327–6331.

[65] J. E. Mondloch, X. Yan, R. G. Finke, *J. Am. Chem. Soc.* **2009**, *131*, 6389–6396.

[66] P. M. Zimmerman, A. Paul, Z. Zhang, C. B. Musgrave, *Inorg. Chem.* **2009**, *48*, 1069–1081.

[67] G. N. Lewis, *Proc. Am. Acad. Arts Sci.* **1905**, *40*, 719–733-.

[68] M. A. Watzky, R. G. Finke, *J. Am. Chem. Soc.* **1997**, *119*, 10382–10400.

[69] D. Nichela, L. Carlos, F. G. Einschlag, *Appl. Catal. B* **2008**, *82*, 11–18.

[70] R. S. Kannan, D. Easwaramoorthy, K. Vijaya, M. S. Ramachandran, *Int. J. Chem. Kinet.* **2008**, *40*, 44–49.

[71] H. N. Miras, C. Mathis, W. Xuan, D.-L. Long, R. Pow, L. Cronin, *PNAS* **2020**, *117*, 10699–10705.

[72] J. McAllister, N. A. G. Bandeira, J. C. McGlynn, A. Y. Ganin, Y.-F. Song, C. Bo, H. N. Miras, *Nat. Commun.* **2019**, *10*, 370.

[73] M. W. Lesley, L. D. Schmidt, *Chem. Phys. Lett.* **1983**, *102*, 459–463.

[74] P. Kepper, I. R. Epstein, K. Kustin, *J. Am. Chem. Soc.* **1981**, *103*, 2133–2134.

[75] M. Orbán, K. Kurin-Csörgei, I. R. Epstein, *Acc. Chem. Res.*, **2015** *48*, 593–601.

[76] R. M. Noyes *J. Phys. Chem.* **1990**, *94*, 4404–4412.

[77] K. Ichimura, *Chem. Rec.* **2002**, *2*, 46–55.

[78] a) H. Ito, *IBM J. Res. Dev.* **1997**, *41*, 119–130; b) E. K. Lin, C. L. Soles, D. L. Goldfarb, B. C. Trinque, S. D. Burns, R. L. Jones, J. L. Lenhart, M. Angelopoulos, C. G. Willson, S. K. Satija, W. L. Wu, *Science* **2002**, *297*, 372–375; c) H. Ito, K. Ichimura, *Macromol. Chem. Phys.* **2000**, *201*, 132–138.

[79] Y. Xu, Q. Chen, Y.-j. Zhao, J. Lv, Z.-h. Li, X.-b. Ma, *Ind. Eng. Chem. Res.* **2014**, *53*, 4207–4214.

[80] H. Ito, C. G. Willson, J. H. J. Frechet, "New UV Resists with Negative or Positive Tone," *1982 Symposium on VLSI Technology. Digest of Technical Papers*, Oiso, Japan, **1982**, 86–87.

[81] K. Arimitsu, K. Ichimura, *Chem. Lett.* **1998**, *27*, 823–824.

[82] S. Kruger, S. Revuru, C. Higgins, S. Gibbons, D. A. Freedman, W. Yueh, T. R. Younkin, R. L. Brainard, *J. Am. Chem. Soc.* **2009**, *131*, 9862–9863.

[83] S. A. Kruger, C. Higgins, B. Cardineau, T. R. Younkin, R. L. Brainard, *Chem. Mater.* **2010**, *22*, 5609–5616.

[84] K. Arimitsu, K. Ichimura, *J. Mater. Chem.* **2004**, *14*, 1164–1172.

[85] K. Arimitsu, H. Kobayashi, M. Furutani, T. Gunji, Y. Abe, *Polym. Chem.* **2014**, *5*, 6671–6677.

[86] L. Guideri, F. De Sarlo, F. Machetti, *Chem. Eu. J.* **2013**, *19*, 665–677.

[87] a) K. Kovacs, R. E. McIlwaine, S. K. Scott, A. F. Taylor, *J. Phys. Chem. A* **2007**, *111*, 549–551; b) P. Warneck, *J. Chem. Educ.* **1989**, *66*, 273.

[88] B. J. Cafferty, A. S. Y. Wong, S. N. Semenov, L. Belding, S. Gmur, W. T. S. Huck, G. M. Whitesides, *J. Am. Chem. Soc.* **2019**, *141*, 8289–8295.

[89] X. Sun, E. V. Anslyn, *Angew. Chem. Int. Ed.* **2017**, *56*, 9522–9526; *Angew. Chem.* **2017**, *129*, 9650–9654.

[90] R. Perry-Feigenbaum, E. Sella, D. Shabat, *Chem. Eur. J.* **2011**, *17*, 12123–12128.

[91] M. S. Baker, S. T. Phillips, *J. Am. Chem. Soc.* **2011**, *133*, 5170–5173.

[92] J. Pallu, C. Rabin, G. Creste, M. Branca, F. Mavre, B. Limoges, *Chem. Eu. J.* **2019**, *25*, 7534–7546.

[93] E. Sella, D. Shabat, *J. Am. Chem. Soc.* **2009**, *131*, 9934–9936.

[94] E. Sella, A. Lubelski, J. Klafter, D. Shabat, *J. Am. Chem. Soc.* **2010**, *132*, 3945–3952.

[95] M. E. Roth, O. Green, S. Gnaim, D. Shabat, *Chem. Rev.* **2016**, *116*, 1309–1352.

[96] P. Scrimin, L. J. Prins, *Chem. Soc. Rev.* **2011**, *40*, 4488–4505.

[97] Q. Wang, T. R. Chan, R. Hilgraf, V. V. Fokin, K. B. Sharpless, M. Finn, *J. Am. Chem. Soc.* **2003**, *125*, 3192–3193.

[98] a) T. R. Chan, R. Hilgraf, K. B. Sharpless, V. V. Fokin, *Org. Lett.* **2004**, *6*, 2853–2855; b) A. K. Feldman, B. Colasson, V. V. Fokin, *Org. Lett.* **2004**, *6*, 3897–3899.

[99] M. D. Hardy, J. Yang, J. Selimkhanov, C. M. Cole, L. S. Tsimring, N. K. Devaraj, *PNAS* **2015**, *112*, 8187–8192.

[100] R. J. Brea, N. K. Devaraj, *Nat. Commun.* **2017**, *8*, 730.

[101] a) E. A. J. Post, S. P. Fletcher, *J. Org. Chem.* **2019**, *84*, 2741–2755; b) E. A. J. Post, A. J. Bissette, S. P. Fletcher, *Chem. Commun.* **2018**, *54*, 8777–8780.

[102] D. Döhler, P. Michael, W. H. Binder, *Acc. Chem. Res.* **2017**, *50*, 2610–2620.

[103] K. J. Singh, A. C. Hoepker, D. B. Collum, *J. Am. Chem. Soc.* **2008**, *130*, 18008–18017.

[104] A. C. Hoepker, L. Gupta, Y. Ma, M. F. Faggin, D. B. Collum, *J. Am. Chem. Soc.* **2011**, *133*, 7135–7151.

[105] L. Gupta, A. C. Hoepker, Y. Ma, M. S. Viciu, M. F. Faggin, D. B. Collum, *J. Org. Chem.* **2013**, *78*, 4214–4230.

[106] F. Barrios-Landeros, B. P. Carrow, J. F. Hartwig, *J. Am. Chem. Soc.* **2008**, *130*, 5842–5843.

[107] A. Hadzovic, D. Song, C. M. MacLaughlin, R. H. Morris, *Organometallics* **2007**, *26*, 5987–5999.

[108] H. Hart, F. A. Cassis, *J. Am. Chem. Soc.* **1954**, *76*, 1634–1639.

[109] K. Arimitsu, K. Ichimura, *J. Mater. Chem.* **2004**, *14*, 336–343.

[110] a) E. R. Thapaliya, S. Swaminathan, B. Captain, F. M. Raymo, *J. Am. Chem. Soc.* **2014**, *136*, 13798–13804; b) P. P. Neelakandan, A. Jiménez, J. D. Thoburn, J. R. Nitschke, *Angew. Chem. Int. Ed.*, **2015**, *54*, 14378–14382.

[111] A. S. Hill, R. S. Shallenberger, *Carbohydr. Res.* **1969**, *11*, 541–545.

[112] V. K. Aggarwal, S. Y. Fulford, G. C. Lloyd-Jones, *Angew. Chem. Int. Ed.* **2005**, *44*, 1706–1708; *Angew. Chem.* **2005**, *117*, 1734–1736.

[113] A. J. Rosenthal, C. G. Overberger, *J. Am. Chem. Soc.* **1960**, *82*, 108–117.

[114] C. N. Rao, S. Hoz, *J. Am. Chem. Soc.* **2011**, *133*, 14795–14803.

[115] Y. Ogata, K. Aoki, *J. Am. Chem. Soc.* **1968**, *90*, 6187–6191.

[116] S. Ephraim, A. E. Woodward, R. B. Mesrobian, *J. Am. Chem. Soc.* **1958**, *80*, 1326–1328.

[117] A. N. Simonov, O. P. Pestunova, L. G. Matvienko, V. N. Parmon, *Kinet. Catal.* **2007**, *48*, 245–254.

[118] R. A. Begum, N. Chanda, T. V. Ramakrishna, P. R. Sharp, *J. Am. Chem. Soc.* **2005**, *127*, 13494–13495.

[119] I. Fabre, N. von Wolff, G. Le Duc, E. Ferrer Flegeau, C. Bruneau, P. H. Dixneuf, A. Jutand, *Chem. Eu. J.* **2013**, *19*, 7595–7604.

[120] K. Soai, T. Shibata, H. Morioka, K. Choji, *Nature* **1995**, *378*, 767–768.

[121] T. Shibata, S. Yonekubo, K. Soai, *Angew. Chem. Int. Ed.* **1999**, *38*, 659–661; *Angew. Chem.* **1999**, *111*, 746–748.

[122] E. Ferrer Flegeau, C. Bruneau, P. H. Dixneuf, A. Jutand, *J. Am. Chem. Soc.* **2011**, *133*, 10161–10170.

[123] L. J. Sewell, G. C. Lloyd-Jones, A. S. Weller, *J. Am. Chem. Soc.* **2012**, *134*, 3598–3610.

[124] D. G. Blackmond, *Proc. Natl. Acad. Sci. USA* **2004**, *101*, 5732–5736.

[125] F. C. Frank, *Biochim. Biophys. Acta* **1953**, *11*, 459–463.

[126] A. H. Alberts, H. Wynberg, *J. Am. Chem. Soc.* **1989**, *111*, 7265–7266.

[127] K. Soai, H. Hori, S. Niwa, *Heterocycles* **1989**, *29*, 2219–2223.

[128] K. Soai, S. Niwa, H. Hori, *J. Chem. Soc. Chem. Commun.* **1990**, 982–983.

[129] A. Matsumoto, T. Abe, A. Hara, T. Tobita, T. Sasagawa, T. Kawasaki, K. Soai, *Angew. Chem. Int. Ed.* **2015**, *54*, 15218–15221; *Angew. Chem.* **2015**, *127*, 15433–15436.

[130] a) G. Ercolani, L. Schiaffino, *J. Org. Chem.* **2011**, *76*, 2619–2626; b) S. V. Athavale, A. Simon, K. N. Houk, S. E. Denmark, *Nat. Chem.* **2020**, *12*, 412–423.

[131] K. Soai, T. Shibata, I. Sato, *Bull. Chem. Soc. Jpn.* **2004**, *77*, 1063–1073.

[132] a) T. Kawasaki, Y. Matsumura, T. Tsutsumi, K. Suzuki, M. Ito, K. Soai, *Science* **2009**, *324*, 492–495; b) A. Matsumoto, H. Ozaki, S. Harada, K. Tada, T. Ayugase, H. Ozawa, T. Kawasaki, K. Soai, *Angew. Chem. Int. Ed.* **2016**, *55*, 15246–15249; *Angew. Chem.* **2016**, *128*, 15472–15475.

[133] N. Chinkov, A. Warm, E. M. Carreira, *Angew. Chem. Int. Ed.* **2011**, *50*, 2957–2961; *Angew. Chem.* **2011**, *123*, 3014–3018.

[134] M. Calvillo-Barahona, J. A. Casares, C. Cordovilla, M. N. Genov, J. M. Martinez-Ilarduya, P. Espinet, *Chem. Eu. J.* **2014**, *20*, 14800–14806.

[135] V. Rautenstrauch, P. Megard, B. Bourdin, A. Furrer, *J. Am. Chem. Soc.* **1992**, *114*, 1418–1428.

[136] M. Mauksch, S. B. Tsogoeva, I. M. Martynova, S. Wei, *Angew. Chem. Int. Ed.* **2007**, *46*, 393–396; *Angew. Chem.* **2007**, *119*, 397–400.

[137] X. Wang, Y. Zhang, H. Tan, Y. Wang, P. Han, D. Z. Wang, *J. Org. Chem.* **2010**, *75*, 2403–2406.

[138] T. Kawasaki, N. Takamatsu, S. Aiba, Y. Tokunaga, *Chem. Commun.* **2015**, *51*, 14377–14380.

[139] S. Miyagawa, S. Aiba, H. Kawamoto, Y. Tokunaga, T. Kawasaki, *Org. Biomol. Chem.* **2019**, *17*, 1238–1244.

ChemSystemsChem

Reviews
doi.org/10.1002/syst.202000026

Chemistry Europe
European Chemical
Societies Publishing

[140] H. J. Yoon, C. A. Mirkin, *J. Am. Chem. Soc.* **2008**, *130*, 11590–11591.

[141] B. Alberts, A. Johnson, J. Lewis, M. Raff, K. Roberts, P. Walter, *Molecular Biology of the Cell. 4th edition*, Garland Science, **2002**.

[142] G. Wulff, F. Diederich, P. Stang, Eds Diederich, F., Stang, PJ. Weinheim: Wiley-VCH **2000**.

[143] J. Rebek, *Supramol. Chem.* **1993**, *1*, 261–266.

[144] W. R. Dichtel, O. S. Miljanic, W. Zhang, J. M. Spruell, K. Patel, I. Aprahamian, J. R. Heath, J. F. Stoddart, *Acc. Chem. Res.* **2008**, *41*, 1750–1761.

[145] J. T. Goodwin, P. Luo, J. C. Leitzel, D. G. Lynn, in *Self-Production of Supramolecular Structures*, (Eds.: G. R. Fleischaker, S. Colonna, P. L. Luisi), Springer, New York, **1994**, pp. 99-104.

[146] T. Tjivikua, P. Ballester, J. Rebek, *J. Am. Chem. Soc.* **1990**, *112*, 1249–1250.

[147] J. S. Nowick, Q. Feng, T. Tjivikua, P. Ballester, J. Rebek, *J. Am. Chem. Soc.* **1991**, *113*, 8831–8839.

[148] F. M. Menger, A. V. Eliseev, N. A. Khanjin, *J. Am. Chem. Soc.* **1994**, *116*, 3613–3614.

[149] E. A. Wintner, M. M. Conn, J. Rebek, *J. Am. Chem. Soc.* **1994**, *116*, 8877–8884.

[150] S. Kamioka, D. Ajami, J. Rebek Jr, *Chem. Commun.* **2009**, 7324–7326.

[151] B. Wang, I. O. Sutherland, *Chem. Commun.* **1997**, 1495–1496.

[152] M. Kindermann, I. Stahl, M. Reimold, M. Pankau, G. von Kiedrowski, *Angew. Chem. Int. Ed. Engl.* **2005**, *44*, 6750–6755.

[153] I. Stahl, G. von Kiedrowski, *J. Am. Chem. Soc.* **2006**, *128*, 14014–14015.

[154] A. Dieckmann, S. Beniken, C. D. Lorenz, N. L. Doltsinis, G. von Kiedrowski, *Chem. Eur. J.* **2011**, *17*, 468–480.

[155] J. M. Quayle, A. M. Z. Slawin, D. Philp, *Tetrahedron Lett.* **2002**, *43*, 7229–7233.

[156] E. Kassianidis, D. Philp, *Angew. Chem. Int. Ed. Engl.* **2006**. *45*, 6344–6348.

[157] I. Bottero, J. Huck, T. Kosikova, D. Philp, *J. Am. Chem. Soc.* **2016**, *138*, 6723–6726.

[158] T. Kosikova, D. Philp, *J. Am. Chem. Soc.* **2017**, *139,* 12579–12590.

[159] J. Huck, T. Kosikova, D. Philp, *J. Am. Chem. Soc.* **2019**, *141*, 13905–13913.

[160] J. M. A. Carnall, C. A. Waudby, A. M. Belenguer, M. C. A. Stuart, J. J. P. Peyralans, S. Otto, *Science* **2010**, *327*, 1502–1506.

[161] S. Kamioka, D. Ajami, J. Rebek Jr., *Proc. Natl. Acad. Sci. USA* **2010**, *107*, 541–544.

[162] T. A. Ploger, G. von Kiedrowski, *Org. Biomol. Chem.* **2014**, *12*, 6908–6914.

[163] T. A. Lincoln, G. F. Joyce, *Science* **2009**, *323*, 1229–1232.

[164] D. H. Lee, J. R. Granja, J. A. Martinez, K. Severin, M. R. Ghadiri, *Nature* **1996**, *382*, 525–528.

[165] X. Li, J. Chmielewski, *Org. Biomol. Chem.* **2003**, *1*, 901–904.

[166] B. Rubinov, N. Wagner, H. Rapaport, G. Ashkenasy, *Angew. Chem. Int. Ed.* **2009**, *48*, 6683–6686; *Angew. Chem.* **2009**, *121*, 6811–6814.

[167] M. Colomb-Delsuc, E. Mattia, J. W. Sadownik, S. Otto, *Nat. Commun.* **2015**, *6*, 7427.

[168] J. W. Sadownik, E. Mattia, P. Nowak, S. Otto, *Nat. Chem.* **2016**, *8*, 264–269.

[169] G. Leonetti, S. Otto, *J. Am. Chem. Soc.* **2015**, *137*, 2067–2072.

[170] F. Wachowius, J. Attwater, P. Holliger, *Q. Rev. Biophys.*, **2017**, *50*, E4.

[171] Y. Baia, A. Chotera, O. Taran, C. Liang, G. Ashkenasy, D. G. Lynn, *Chem. Soc. Rev.* **2018**, *47*, 5444–5456.

[172] a) T. Achilles, G. von Kiedrowski, *Angew. Chem. Int. Ed.* **1993**, *32*, 1198–1201; *Angew. Chem.* **1993**, *105*, 1225–1228.

[173] T. A. Lincoln, G. F. Joyce, *Science* **2009**, *323*, 1229–1232.

[174] N. Vaidya, M. L. Manapat, I. A. Chen, R. Xulvi-Brunet, E. J. Hayden, N. Lehman, *Nature* **2012**, *491*, 72–77.

[175] a) I. A. Chen, R. W. Roberts, J. W. Szostak, *Science* **2004**, *305*, 1474–1476; b) K. Adamala, J. W. Szostak, *Science* **2013**, *342*, 1098–1100.

[176] a) N. Prywes, J. C. Blain, F. Del Frate, J. W. Szostak, *Elife* **2016**, *5*, e17756; b) T. Walton, W. Zhang, L. Li, C. P. Tam, J. W. Szostak, *Angew. Chem. Int. Ed.* **2019**, *58*, 10812–10819.

[177] R. Issac, J. Chmielewski, *J. Am. Chem. Soc.* **2002**, *124*, 6808–6809.

[178] D. H. Lee, K. Severin, Y. Yokobayashi, M. R. Ghadiri, *Nature* **1997**, *390*, 591–594.

[179] a) G. Ashkenasy, R. Jagasia, M. Yadav, M. R. Ghadiri, *Proc. Natl. Acad. Sci. USA* **2004**, *101*, 10872–10877; b) Z. Dadon, N. Wagner, G. Ashkenasy, *Angew. Chem. Int. Ed.* **2008**, *47*, 6128–6136; *Angew. Chem.* **2008**, *120*, 6221–6230; c) Z. Dadon, N. Wagner, S. Alasibi, M. Samiappan, R. Mukherjee, G. Ashkenasy, *Chem. Eu. J.* **2015**, *21*, 648–654.

[180] B. Rubinov, N. Wagner, M. Matmor, O. Regev, N. Ashkenasy, G. Ashkenasy, *ACS Nano* **2012**, *6*, 7893–7901.

[181] J. Shorter, S. Lindquist, *Nat. Rev. Genet.* **2005**, *6*, 435–450.

[182] R. J. Pearson, E. Kassianidis, A. M. Slawin, D. Philp, *Chem. Eur. J.* **2006**, *12*, 6829–6840.

[183] A. A. Pogodaev, C. L. Fernandez Regueiro, M. Jakstaite, M. J. Hollander, W. T. S. Huck, *Angew. Chem. Int. Ed.* **2019**, *58*, 14539–14543.

[184] a) A. Eschenmoser, *Tetrahedron* **2007**, *63*, 12821–12844; b) B. H. Patel, C. Percivalle, D. J. Ritson, C. D. Duffy, J. D. Sutherland, *Nat. Chem.* **2015**, *7*, 301–307; c) J. D. Sutherland, *Nat. Rev. Chem.* **2017**, *1*, 0012.

[185] J. B. Lambert, S. A. Gurusamy-Thangavelu, K. B. A. Ma, *Science* **2010**, *327*, 984–986.

[186] a) C. M. Gothard, S. Soh, N. A. Gothard, B. Kowalczyk, Y. H. Wei, B. Baytekin, B. A. Grzybowski, *Angew. Chem. Int. Ed.* **2012**, *51*, 7922–7927; *Angew. Chem.* **2012**, *124*, 8046–8051; b) T. Klucznik, B. Mikulak-Klucznik, M. P. McCormack, H. Lima, S. Szymkuć, M. Bhowmick, K. Molga, Y. Zhou, L. Rickershauser, E. P. Gajewska, A. Toutchkine, P. Dittwald, M. P. Startek, G. J. Kirkovits, R. Roszak, A. Adamski, B. Sieredzińska, M. Mrksich, S. L. J. Trice, B. A. Grzybowski, *Chem.* **2018**, *4*, 522–532; c) M. D. Bajczyk, P. Dittwald, A. Wolos, S. Szymkuc, B. A. Grzybowski, *Angew. Chem. Int. Ed.* **2018**, *57*, 2367–2371; *Angew. Chem.* **2018**, *130*, 2391–2395.

[187] M. M. Lerch, A. Grinthal, J. Aizenberg, *Adv. Mater.* **2020**, *32*, 1905554.

[188] a) J. A. Pojman, *J. Am. Chem. Soc.* **1991**, *113*, 6284–6286; b) J. A. Pojman, G. Curtis, V. M. Ilyashenko, *J. Am. Chem. Soc.* **1996**, *118*, 3783–3784; c) E. Jee, T. Bansagi Jr., A. F. Taylor, J. A. Pojman, *Angew. Chem.* **2016**, *128*, 2167–2171; *Angew. Chem. Int. Ed.* **2016**, *55*, 2127–2131.

[189] S. N. Semenov, A. S. Y. Wong, R. M. van der Made, S. G. J. Postma, J. Groen, H. W. H. van Roekel, T. F. A. de Greef, W. T. S. Huck, *Nat. Chem.* **2015**, *7*, 160–165.

[190] a) A. M. Turing, *Philos. Trans. R. Soc. London Ser. B* **1952**, *237*, 37–72; b) P. De Kepper, J. Horvath, I. Szalai, *Science* **2009**, *324*, 772–775.

[191] Z. Tan, S. Chen, X. Peng, L. Zhang, C. Gao, *Science* **2018**, *360*, 518–521.

[192] X. M. He, M. Aizenberg, O. Kuksenok, L. D. Zarzar, A. Shastri, A. C. Balazs, J. Aizenberg, *Nature* **2012**, *487*, 214–218.

REVIEWS

Across the board: Autocatalysis has broad importance ranging from photolithography to the origins of life. This Review covers all main aspects of autocatalysis. It introduces the kinetics of autocatalysis, describes mechanisms for the major classes of autocatalytic reactions, highlights the concept of autocatalytic reaction networks, proposes approaches for designing new autocatalytic systems, and discusses challenges and perspectives in the field of autocatalysis.

A. I. Hanopolskyi, V. A. Smaliak, A. I. Novichkov, Dr. S. N. Semenov*

Autocatalysis: Kinetics, Mechanisms and Design